The Endogenous Grid Method for Discrete-Continuous Dynamic Choice Models with (or without) Taste Shocks †

Fedor Iskhakov
Australian National University and CEPAR UNSW
Thomas H. Jørgensen
University of Copenhagen
John Rust
Georgetown University
Bertel Schjerning
University of Copenhagen

September 2016

Abstract: We present a fast and accurate computational method for solving and estimating a class of dynamic programming models with discrete and continuous choice variables. The solution method we develop for structural estimation extends the endogenous gridpoint method (EGM) to discrete-continuous (DC) problems. Discrete choices can lead to kinks in the value functions and discontinuities in the optimal policy rules, greatly complicating the solution of the model. We show how these problems are ameliorated in the presence of additive choice-specific *IID* extreme value taste shocks which are typically interpreted as "unobserved state variables" in structural econometric applications, or serve as "random noise" to smooth out kinks in the value functions in numerical applications. We present Monte Carlo experiments that demonstrate the reliability and efficiency of the DC-EGM and the associated Maximum Likelihood estimator for structural estimation of a life cycle model of consumption with discrete retirement decisions.

Keywords: Lifecycle model, discrete and continuous choice, retirement choice, endogenous gridpoint method, nested fixed point algorithm, extreme value taste shocks, smoothed max function, structural estimation.

JEL classification: C13, C63, D91

† We acknowledge helpful comments from Chris Carroll and *many other people*, participants at seminars at UNSW, University og Copenhagen, the 2012 conferences of the Society of Economic Dynamics, the Society for Computational Economics, the Initiative for Computational Economics at Zurich (ZICE 2014, 2015). This paper is part of the IRUC research project financed by the Danish Council for Strategic Research (DSF). Iskhakov, Rust and Schjerning gratefully acknowledge this support. Iskhakov gratefully acknowledges the financial support from the Australian Research Council Centre of Excellence in Population Ageing Research (project number CE110001029) and Michael P. Keane's Australian Research Council Laureate Fellowship (project number FL110100247). Jørgensen gratefully acknowledges financial support from the Danish Council for Independent Research in Social Sciences (FSE, grant no. 4091-00040). **Correspondence address:** Research School of Economics, ANU College of Business and Economics, 1018 HW Arndt building, The Australian National University, Canberra, ACT 0200 phone: (+61)261256193, email: `fedor.iskhakov@anu.edu.au`

1 Introduction

This paper develops a fast new solution algorithm for structural estimation of dynamic programming models with discrete and continuous choices. The algorithm we propose extends the Endogenous Grid Method (EGM) by Carroll (2006) to discrete-continuous (DC) models. We refer to it as the DC-EGM algorithm. We embed the DC-EGM algorithm in the inner loop of the nested fixed point (NFXP) algorithm (Rust, 1987), and show that the resulting maximum likelihood estimator produces accurate estimates of the structural parameters at low computational cost.

A classic example of a DC model is a life cycle model with discrete retirement and continuous consumption decisions. While there is a well developed literature on solution and estimation of dynamic discrete choice models, and a separate literature on estimation of life cycle models without discrete choices, there has been far less work on solution and estimation of DC models.[1]

There is good reason why DC models are much less commonly seen in the literature: they are substantially harder to solve. The value functions of models with only continuous choices are typically concave and the optimal policy function can be found from the *Euler equation*. EGM avoids the need to numerically solve the nonlinear Euler equation for the optimal continuous choice at each grid point in the state space. Instead, EGM specifies an exogenous grid over an endogenous quantity, e.g. savings, to analytically calculate the optimal policy rule, e.g., consumption, and endogenously determine the pre-decision state, e.g., beginning-of-period resources.[2] DC-EGM retains the main desirable properties of EGM, namely it avoids the bulk of root-finding operations and handles borrowing constraints in an efficient manner.

Dynamic programs that have only discrete choices are substantially easier to solve, since the optimal decision rule is simply the alternative with highest choice-specific value. However, solving dynamic programming problems that combine continuous and discrete choices is substantially more complicated, since discrete choices introduce kinks and non-concave regions in the value

[1] There are relatively few examples of *structural estimation* or *numerical solution* of DC models. Some prominent examples include the model of optimal non-durable consumption and housing purchases (Carroll and Dunn, 1997), optimal saving and retirement (French and Jones, 2011), and optimal saving, labor supply and fertility (Adda, Dustmann and Stevens, forthcoming).

[2] The EGM is in fact a specific application of what is referred to as "controlling the post-decision state" in operations research and engineering (Bertsekas, Lee, van Roy and Tsitsiklis, 1997). Carroll (2006) introduced the idea in economics by developing the EGM algorithm with the application to the buffer-stock precautionary savings model. Since then the idea became widespread in economics. Further generalizations of EGM include Barillas and Fernández-Villaverde (2007); Hintermaier and Koeniger (2010); Ludwig and Schön (2013); Fella (2014); Iskhakov (2015). Jørgensen (2013) compares the performance of EGM to Mathematical Programming with Equilibrium Constraints (MPEC).

function that lead to discontinuities in the policy function of the continuous choice (consumption). This can lead to situations where the Euler equation has *multiple solutions* for consumption, and hence it is only a *necessary* rather than a sufficient condition for the optimal consumption rule (Clausen and Strub, 2013). This inherent feature of DC problems complicates any method one might consider for solving DC models.

We illustrate how DC-EGM can deal with these inherent complications using a life cycle model with a continuous consumption and binary retirement choice with and without taste shocks. Our example is a simple extension of the classic life cycle model of Phelps (1962) where, in the absence of a retirement decision, the optimal consumption rule could hardly be any simpler — a linear function of resources. However, once the discrete retirement decision is added to the Phelp's problem — in our case allowing a worker with logarithmic utility to also make a binary irreversible retirement decision — the consumption function becomes unexpectedly complex, with multiple discontinuities in the optimal consumption rule. We derive an *analytic solution* for this model, use it to demonstrate the accuracy of the solution obtained numerically by DC-EGM, and then investigate the performance of the Rust's NFXP type nested estimator based on the DC-EGM solution algorithm to estimate the structural parameters of this model.

Fella (2014) showed how EGM could be adapted to solve non-concave problems, including models with discrete and continuous choices. In this paper we focus on discrete choices and show that introducing *IID* Extreme Value Type I choice-specific taste shocks not only facilitates maximum likelihood estimation, but also smooths out some of the kinks in the value functions thereby simplifying the numerical solution of the model. This approach results in *multinomial logit formulas* for the *conditional choice probabilities* for the discrete choices and a closed form expression for the expectation of the value function with respect to these taste shocks.[3]

In econometric applications continuously distributed taste shocks are essential for generating predictions from dynamic programming models that are *statistically non-degenerate*. Such predictions assign a positive (however small) choice probability to *every* alternative, and therefore preclude zero likelihood observations. These shocks are interpreted as *unobserved state variables*, i.e. idiosyncratic shocks observed by agents but not by the econometrician. However, in numerical

[3]In principle, the Extreme Value assumption could be relaxed to allow for other distributions at the cost of numerical approximation of choice probabilities and the conditional expectation of the value function. For example, Bound, Stinebrickner and Waidmann (2010), assume that the discrete choice specific taste shocks are Normal rather than Extreme Value. Yet, we follow the long tradition of discrete choice modeling dating back to (McFadden, 1973) and (Rust, 1987).

or theoretical applications taste shocks can serve as a smoothing device (homotopy perturbation) that facilitates the numerical solution of more advanced DC models that may have excessively many kinks and discontinuities, for example caused by a large number of discrete choices.

The inclusion of Extreme Value Type I taste shocks have a long history in discrete choice modeling dating back to the seminal work by McFadden (1973). This assumption is typically invoked in microeconometric analyses of dynamic discrete choice models where numerical performance boosted by closed form choice probabilities is particularly important, see for example Rust (1994) and the recent survey by Aguirregabiria and Mira (2010). Some recent studies of DC models with Extreme Value taste shocks include Casanova (2010); Ejrnæs and Jørgensen (2015); Iskhakov and Keane (2016); Oswald (2016) and Adda, Dustmann and Stevens (forthcoming).

At first glance, the addition of stochastic shocks would appear to make the problem *harder* to solve, since both the optimal discrete and continuous decision rules will necessarily be functions of these stochastic shocks. However, we show that a variety of stochastic variables in DC models *smooth out* many of the kinks in the value functions and the discontinuities in the optimal consumption rules. In the absence of smoothing, we show that every kink induced by the comparison of the discrete choice specific value functions in any period t propagates backwards in time to all previous periods as a manifestation of the decision maker's anticipation of the future discrete action. The resulting accumulation of kinks during backward induction presents the most significant challenge for the numerical solution of DC models. In presence of taste shocks the decision maker can only anticipate a particular future discrete action to be more or less probable, and thus the primary reason for the accumulation of kinks disappears. Thus, the combination of taste shocks and the stochastic variables in the model is perhaps the most powerful device to prevent the propagation and accumulation of kinks.[4]

In the case where Extreme Value taste shocks are used as a logit *smoothing device* of an underlying deterministic model of interest, we show that the latter problem can be approximated by the smoothed model to any desirable degree of precision. The scale parameter $\sigma \geq 0$ of the corresponding Extreme Value distribution then serves as a *homotopy* or *smoothing* parameter. When σ is sufficiently large, the non-concave regions near the kinks in the non-smoothed value function disappear and the value functions become globally concave. But even small values of

[4]Contrary to the macro literature that uses stochastic elements such as employment lotteries (Rogerson, 1988; Prescott, 2005; Ljungqvist and Sargent, 2005) to smooth out non-convexities, the taste shock we introduce in DC models in general *do not* fully convexify the problem.

σ smooth out many of the kinks in the value functions and suppress their accumulation in the process of backward induction as noted above. An additional benefit of the taste shocks is that standard integration methods, such as quadrature rules, apply when the expected value function is a smooth function.

We run a series of Monte Carlo simulations to investigate the performance of DC-EGM for structural estimation of the life cycle model with the discrete retirement decision. We find that a maximum likelihood estimator that nests the DC-EGM algorithm performs well. It quickly produces accurate estimates of the structural parameters of the model even when fairly coarse grids over wealth are used. We find the cost of "oversmoothing" to be negligible in the sense that the parameter estimates of a perturbed model with stochastic taste shocks are estimated very accurately even if the true model does not have taste shocks. Thus, even in the case where the addition of taste shocks results in a *misspecification* of the model, the presence of these shocks improves the accuracy of the solution and reduces computation time without increasing the approximation bias significantly. Even when very few grid points are used to solve the model, we find that smoothing the problem improves the root mean square error (RMSE). Particularly, with an appropriate degree of smoothing (σ), we can reduce the number of gridpoints by an order of magnitude without much increase in the RMSE of the parameter estimates.

DC-EGM is applicable to many fields of economics and has been implemented in several recent empirical applications. Ameriks, Briggs, Caplin, Shapiro and Tonetti (2015) study how the need for long term care and bequest motive interact with government-provided support to shape the wealth profile of the elderly. They use an endogenous grid method similar to DC-EGM to solve and estimate the corresponding non-concave model. Iskhakov and Keane (2016) employ DC-EGM to estimate a life-cycle model of discrete labor supply, human capital accumulation and savings for the Australian population. They use the model to evaluate Australia's defined contribution pension scheme with means-tested minimal pension, and quantify the effects of anticipated and unanticipated policy changes. Yao, Fagereng and Natvik (2015) use DC-EGM to analyze how housing and mortgage debt affects consumer's marginal propensity to consume. They estimate a model in which households hold debt, financial assets and illiquid housing and find that a substantial fraction of households are likely to behave in a "hand-to-mouth" fashion despite having significant wealth holdings. Druedahl and Jørgensen (2015) employ a modified version of DC-EGM to analyze the credit card debt puzzle. They solve a model of optimal consumption and debt

holdings and show how, for some parameterizations of the model, a large group of consumers find it optimal to simultaneously hold positive gross debt and positive gross assets even though the interest rate on the debt is much higher than the rate on the assets. Ejrnæs and Jørgensen (2015) use DC-EGM to estimate a model of optimal consumption and saving with a fertility choice to analyze the saving behavior around intended and unintended childbirths. They model the fertility process as a discrete choice over effort to conceive a child subject to a biological fecundity constraint and allow for the possibility of unintended child births through imperfect contraceptive control.

In the next section we present a simple extension of the life cycle model of consumption and savings with logarithmic utility studied by Phelps (1962) where we allow for a discrete retirement decision. We derive a closed-form solution to this problem, and discuss its properties. Using this simple model we demonstrate the accuracy of the deterministic version of DC-EGM. We then introduce extreme value taste shocks and show how the implied smoothing affects the value functions and the optimal policy rules. In particular, we show that the error introduced by "extreme value smoothing" is uniformly bounded, and prove that the solution of the smoothed DP problem with taste shocks converges to the solution to the DP problem without taste shocks as scale of the shocks approaches zero. Section 3 presents the full DC-EGM algorithm. In section 4 we show how it is incorporated in the Nested Fixed Point algorithm for maximum likelihood estimation of the structural parameters in the retirement model. We present the results of a series of Monte Carlo experiments in which we explore the performance of the estimator in a variety of settings. We conclude with a short discussion of the range of models that DC-EGM is applicable to and discuss some open issues with this method.

2 An Illustrative Problem: Consumption and Retirement

This section extends the classic life-cycle consumption/savings model of Phelps (1962) to allow a discrete retirement decision. We derive an analytic solution to this problem with logarithmic utility to both illustrate the complexity caused by the addition of a discrete retirement choice and show how DC-EGM finds this solution. While we focus on this simple example for expositional clarity, DC-EGM can be applied to a much more general class of problems that include taste and income shocks. We will discuss these extensions in section 3 and show how the addition of shocks can actually simplify the solution of the model using DC-EGM.

2.1 Deterministic model of consumption/savings and retirement

Consider the discrete-continuous (DC) dynamic optimization problem

$$\max_{\{c_t,d_t\}_{t=1}^{T}} \sum_{t=1}^{T} \beta^t(\log(c_t) - \delta d_t) \tag{1}$$

involving choice of consumption c_t and when to retire to maximize discounted utility, where $d_t = 0$ denotes retirement and $d_t = 1$ continued work and $\delta > 0$ is the disutility of work. We assume retirement is absorbing, i.e. a retiree cannot to return to work.

We solve (1) subject to a sequence of period-specific borrowing constraints, $c_t \leq M_t$, where $M_t = R(M_{t-1} - c_{t-1}) + yd_{t-1}$ is the consumer's resources at the beginning of period t. There is a fixed, non-stochastic gross interest rate, R, and labor income y for workers. The continuous consumption decision and discrete retirement decision are made at the start of each period, whereas interest earnings and labor income are paid at the end of the period. This timing convention is standard in the literature and is the appropriate when we extend the model in the next section to a much wider class of problems where R and y are random variables.

Let $V_t(M, 1)$ and $V_t(M, 0)$ be the expected discounted lifetime utility of a worker and retiree, respectively, in period t of their life. The choice problem of the worker can be expressed recursively through the Bellman equation

$$V_t(M, 1) = \max\{v_t(M, 0), v_t(M, 1)\}, \tag{2}$$

where the *choice-specific value functions* are given as

$$v_t(M, 0) = \max_{0\leq c\leq M} \{\log(c) + \beta V_{t+1}\big(R(M - c), 0\big)\}, \tag{3}$$

$$v_t(M, 1) = \max_{0\leq c\leq M} \{\log(c) - \delta_t + \beta V_{t+1}\big(R(M - c) + y_{t+1}, 1\big)\}. \tag{4}$$

The value function for a retiree $V_t(M, 0)$ has a closed-form solution given by Phelps (1962, p. 742), so we focus on deriving formulas for $v_t(M, 1)$ and finding the optimal consumption rule $c_t(M, 1)$ for a worker who has the option to either retire or continue working.

Note that even if $v_t(M, 0)$ and $v_t(M, 1)$ are concave functions of M, the value function $V_t(M, d)$ is the maximum of these two concave functions and will generally not be globally concave

(Clausen and Strub, 2013). Further $V_t(M,1)$ will generally have a *kink point* at the value $M = \overline{M}_t$ where the two choice-specific value functions cross: $v_t(\overline{M}_t, 1) = v_t(\overline{M}_t, 0)$. We refer to these as *primary kinks* since they constitute *optimal retirement thresholds* for the worker, i.e. $d_t(M) = 1$ if $M < \overline{M}_t$ and $d_t(M) = 0$ if $M \geq \overline{M}_t$.

The worker is indifferent between retiring and working at the primary kink $\overline{M}_t$ and $V_t(M,1)$ is non-differentiable at this point. However the left and right hand derivatives, V_t^- and V_t^+, exist and satisfy $V_t^-(\overline{M}_t, 1) < V_t^+(\overline{M}_t, 1)$. The discontinuity in the derivative of $V_t(M,1)$ at $\overline{M}_t$ leads to a discontinuity in the optimal consumption function in the *previous* period $t-1$ because the Bellman equation for $V_{t-1}(M,1)$ depends on $V_t(M,1)$, so the primary kink in the latter results in a *secondary kink* in $V_{t-1}(M,1)$. Thus, the primary kinks propagate back in time and manifest themselves in an accumulation of secondary kinks in the value functions in earlier periods, resulting in a increasing number of discontinuities in the consumption functions in earlier periods of the life cycle. The jumps in consumption are caused by the worker's desire to increase saving for an *anticipated retirement* at some point in the future.

Theorem 1 (Analytical solution to the retirement problem)**.** *Assume that income and disutility of work are time-invariant and the discount factor β and the disutility of work δ are not too large, i.e.*

$$\beta R \leq 1 \text{ and } \delta < (1+\beta)\log(1+\beta). \tag{5}$$

Then $\tau \in \{1, \ldots, T\}$ the optimal consumption rule in the workers' problem (2)-(4) *is given by*

$$c_{T-\tau}(M,1) = \begin{cases} M & \text{if } M \leq y/R\beta, \\ [M + y/R]/(1+\beta) & \text{if } y/R\beta \leq M \leq \overline{M}_{T-\tau}^{l_1}, \\ [M + y(1/R + 1/R^2)]/(1+\beta+\beta^2) & \text{if } \overline{M}_{T-\tau}^{l_1} \leq M \leq \overline{M}_{T-\tau}^{l_2}, \\ \ldots & \ldots \\ \left[M + y\left(\sum_{i=1}^{\tau-1} R^{-i}\right)\right]\left(\sum_{i=0}^{\tau-1}\beta^i\right)^{-1} & \text{if } \overline{M}_{T-\tau}^{l_{\tau-2}} \leq M \leq \overline{M}_{T-\tau}^{l_{\tau-1}}, \\ [M + y\left(\sum_{i=1}^{\tau} R^{-i}\right)]\left(\sum_{i=0}^{\tau}\beta^i\right)^{-1} & \text{if } \overline{M}_{T-\tau}^{l_{\tau-1}} \leq M < \overline{M}_{T-\tau}^{r_{\tau-1}}, \\ \left[M + y\left(\sum_{i=1}^{\tau-1} R^{-i}\right)\right]\left(\sum_{i=0}^{\tau}\beta^i\right)^{-1} & \text{if } \overline{M}_{T-\tau}^{r_{\tau-1}} \leq M < \overline{M}_{T-\tau}^{r_{\tau-2}}, \\ \ldots & \ldots \\ [M + y(1/R + 1/R^2)]\left(\sum_{i=0}^{\tau}\beta^i\right)^{-1} & \text{if } \overline{M}_{T-\tau}^{r_2} \leq M < \overline{M}_{T-\tau}^{r_1}, \\ [M + y/R]\left(\sum_{i=0}^{\tau}\beta^i\right)^{-1} & \text{if } \overline{M}_{T-\tau}^{r_1} \leq M < \overline{M}_{T-\tau}, \\ M\left(\sum_{i=0}^{\tau}\beta^i\right)^{-1} & \text{if } M \geq \overline{M}_{T-\tau}. \end{cases} \tag{6}$$

The segment boundaries are totally ordered with

$$y/R\beta < \overline{M}_{T-\tau}^{l_1} < \cdots < \overline{M}_{T-\tau}^{l_{\tau-1}} < \overline{M}_{T-\tau}^{r_{\tau-1}} < \cdots < \overline{M}_{T-\tau}^{r_1} < \overline{M}_{T-\tau}, \tag{7}$$

and the right-most threshold $\overline{M}_{T-\tau}$ *given by*

$$\overline{M}_{T-\tau} = \frac{(y/R)e^{-K}}{1-e^{-K}}, \text{ where } K = \delta\left(\sum_{i=0}^{\tau}\beta^i\right)^{-1}, \tag{8}$$

defines the smallest level of wealth sufficient to induce the consumer to retire at age $t = T - \tau$.

The proof of Theorem 1 is available on request, though we will show how this solution is derived when we introduce the DC-EGM algorithm in the next subsection.[5] It establishes that the optimal consumption rule (6) is piece-wise linear in M, and in period t consists of $2(T-t)+1$ segments. The first segment where $M < y/R\beta$ is the credit constrained region. The next $T-t-1$ segments are demarcated by the *liquidity constraint kink points* $\overline{M}_t^{l_j}$ which define values of M at which the consumer is liquidity constrained at age $t+j$ but not at any earlier age. The remaining segments are defined by the secondary kinks, $\overline{M}_t^{r_j}$, $j = 1, \ldots, T-t-1$ and represent the largest level of saving for which it is optimal to retire at age $t+j$ but not at any earlier age. The optimal consumption function is discontinuous at points $\overline{M}_t^{r_j}$, and including the discontinuity at the retirement threshold $\overline{M}_t$ there are a total of $T-t$ downward jumps in $c_t(M,1)$.

Theorem 1 implies that the value function $V_t(M,1)$ is piecewise logarithmic with the same kink points, and can be written as $V_t(M,1) = B_t \log(c_t(M,1)) + C_t$ for constants (B_t, C_t) that depend on the region M falls in. $V_t(M,1)$ has one primary kink at the optimal retirement threshold $\overline{M}_t$ and $T-t-1$ secondary kinks at $\overline{M}_t^{r_j}$, $j = 1, \ldots, T-t-1$, and $T-t$ kinks related to current period and future liquidity constraints at $M = y/R\beta$ and $\overline{M}_t^{l_j}$, $j = 1, \ldots, T-t-1$. If $R\beta = 1$ the liquidity-related kink points collapse to a single point $M = y/R\beta = y = \overline{M}_t^{l_1} = \cdots = \overline{M}_t^{l_{T-t-1}}$.

[5] Note that the assumptions on the parameters β, δ and R are needed to ensure the ordering of the bounderies (7). Modified versions of Theorem 1 hold under weaker conditions, including a version where income and the disutility of work are age-dependent. However, depending on the paths of income and disutility of work some of the intermediate thresholds in Theorem 1 may not exist, or may be equal to each other.

2.2 DC-EGM for problems without taste shocks

We are now in a position to introduce a generalization of the EGM algorithm for solving discrete-continuous problems that we call the DC-EGM algorithm. We describe DC-EGM by showing how it can be used to solve for the optimal consumption rule in Theorem 1. After explaining the procedure, we compare its numerical performance by showing how closely DC-EGM can approximate the analytic solution in Theorem 1.

DC-EGM is a backward induction algorithm that uses the *Euler equation* to sequentially compute the choice-specific value functions $v_t(M, d)$ and the corresponding consumption functions $c_t(M, d)$ starting at the last period of life, T. We use DC-EGM to solve the three last periods of the consumption-retirement of section 2.1. However before we do this, note that in a generic period t of the backward induction, the Bellman equation (4) for the optimal consumption of a worker implies the following first order condition known as the Euler equation

$$\begin{aligned} 0 &= u'(c) - \beta R u'(c_{t+1}(R(M-c)+y, 1)) \\ &= 1/c - \frac{\beta R}{c_{t+1}(R(M-c)+y, 1)}. \end{aligned} \tag{9}$$

Similarly the Bellman equation (3) implies the following Euler equation for a retiree

$$\begin{aligned} 0 &= u'(c) - \beta R u'(c_{t+1}(R(M-c), 0)) \\ &= 1/c - \frac{\beta R}{c_{t+1}(R(M-c), 0)}, \end{aligned} \tag{10}$$

where the first equation in (9) and (10) shows the general case for a general concave $u(c)$, and the second equation shows the specialzation to the case $u(c) = \log(c)$. The solutions to these Euler equations are the period t choice-specific consumption functions, $c_t(M, d)$. As is well known, in the final period of life, T the optimal consumption rule is $c_T(M, d) = M$ and if there is positive disutility of working, all workers will retire (i.e. $\overline{M}_T = 0$) since income is paid at the *end* of the period after the person has died, so it follows that $d_T(M) = 0$.

Now consider a retiree in period $T-1$. The Euler equation (10) implies the following closed-form solution $c_{T-1}(M, 0) = M/(1+\beta)$. Consider how this solution is computed using the original EGM algorithm by Carroll (2006), which is applicable since there are no further discrete decisions given our assumption that retirement is an absorbing state. EGM uses the Euler equation (10)

to construct an *endogenous grid over* M from an *exogenous grid over savings* A ($A = M - c$). Let $\vec{A} = \{A_1, \ldots, A_J\}$ denote the exogenous grid over savings. For each saving grid point A_j, the Euler equation (10) can be *analytically solved* in cases where $u'(c)$ is *analytically invertible.* This is true in the case where $u(c) = \log(c)$, and the solution is easily seen to be $c_{T-1}(M_j, 0) = A_j/\beta$, where M_j is an element of the endogenous grid $\vec{M}$ implied the exogenous grid over savings $\vec{A}$. We have $M_j = A_j + c_{T-1}(M_j, 0) = A_j(1 + 1/\beta)$, which implies the solution $c_{T-1}(M_j, 0) = M_j/(1 + \beta)$.

Thus, EGM produces the exact solution in this particular case. In other problems where the optimal consumption rule might not be linear, EGM results in a piece-wise linear approximation to the nonlinear consumption function produced by interpolating the solution for consumption at the endogenous grid points as described above. The key to the use of EGM is the ability to *analytically invert marginal utility* $u'(c)$ to solve for c in a single evaluation as a function of A_j rather than M, *bypassing the need to solve the nonlinear Euler equation for c as a function of M.* Thus in the case of a general $u(c)$ function we have

$$c_t(A_j, 0) = u'^{-1}\left(R\beta u'(c_{t+1}(RA_j, 0))\right) \tag{11}$$

which implies the following endogenous gridpoint $M_j = A_j + c_t(A_j, 0)$. Thus, EGM has computed $c_t(M_j, 0)$ at the endogenous gridpoint M_j without any need for numerical root-finding (e.g. Newton's method) required by methods that directly solve the Euler equation (10) for c_t at each M_j in an exogenous grid over M.

Now consider a worker in period $T - 1$. The worker must solve for *two consumption functions* $c_{T-1}(M, 0)$ and $c_{T-1}(M, 1)$ corresponding to the decision to retire or not retire, respectively. However no special complications are created at this point: we simply apply "standard EGM" to solve for the optimal consumption rule of a worker, $c_{T-1}(M, 1)$, using the Euler equation (9) just as we described for the case of a retiree above. This also results in a closed form solution $c_{T-1}(M, 1) = (M + y/R)/(1 + \beta)$. However we also need to take care to ensure that liquidity constraint $c_{T-1} \leq M$ is satisfied, so we actually have $c_{T-1}(M, 1) = M$ for $M \leq y/R\beta$. Thus, we have already verified that EGM can find the *exact solution* at least in period $T - 1$, since it matches the first two segments of the true solution $c_{T-1}(M, 1)$ given in equation (6) of Theorem 1.

In summary, when there are discrete choices, DC-EGM invokes the EGM algorithm to calculate, via simple linear interpolation as described above, piece-wise linear approximations *decision-specific consumption functions* $c_t(M_j(d), d)$ defined over *decision-specific endogenous grids*

$\vec{M}(d) = \{M_1(d), \ldots, M_J(d)\}$. However what is different about DC-EGM is that we need to use the Bellman equations (3) and (4) to construct piece-wise linear approximations to $v_t(M, 0)$ and $v_t(M, 1)$ by linear interpolation over the respective endogenous grids $\vec{M}(0)$ and $\vec{M}(1)$. Using the interpolated decision-specific value functions, we then find the optimal retirement threshold (primary kink) $\overline{M}_t$ by finding the point of intersection of the two decision-specific value functions, $v_t(M, 0)$ and $v_t(M, 1)$ and returns $V_t(M, d)$ as the *upper envelope* of these decision-specific value functions.

So far DC-EGM seems to be a rather straightforward extension of standard EGM, but at period $T - 2$ we encounter an important additional complication: the *emergence of secondary kinks* that result in *multiple local optima for c*. Recall that $V_t(M, 1)$ is the maximum of decision-specific value functions, and is not globally concave. In particular, $V_{T-1}(M, 1)$ will have a *non-concave region* near $\overline{M}_{T-1}$, where the decision-specific value functions $v_{T-1}(M, 0)$ and $v_{T-1}(M, 1)$ cross. This implies that at time $T - 2$ when we search over c to maximize $\log(c) + \beta V_{T-1}(R(M - c) + y, 1)$ there will be a non-concave region for values of $R(M - c) + y$ near $\overline{M}_{T-1}$. In the non-concave region there are multiple local optima for c with corresponding multiple solutions to the Euler equations (which are simply the first order conditions corresponding to the decision-specific value functions). Thus, DC-EGM must also take care to select the *correct solution to the Euler equation* corresponding to the globally optimal consumption value in cases where the Euler equation has multiple solutions. This is achieved by the calculation of the *upper envelope* of separate segments of the decision-specific value functions that appear near the secondary kinks. This leads to an elimination of *dominated grid points* and a merging of the remaining endogenous gridpoints in a way we describe below.

To illustrate how this works we refer the reader to figure 1 which illustrates the operation of DC-EGM at period $T - 2$ of a problem where $T = 20$, $R = 1$, $\beta = 0.98$, $\delta = 1$, and $y = 20$. In period $T - 1$ the primary kink is $\overline{M}_{T-1} = 30.4382$, and the top left panel (a) we plot discounted utilities $\log(c) + \beta V_{T-1}(R(M - c) + y)$ in period $T - 2$ for different values of M, and we see how the primary kink in $V_{T-2}(M, 1)$ at $\overline{M}_{T-1}$ results in a secondary kink and a non-concave region in the value of consumption at $T - 2$ at various points c depending on the value of M. For example the lowest dotted line plots $\log(c) + \beta V_{T-1}(R(M - c) + y, 1)$ for $M = 28$ and we see that the primary kink at $\overline{M}_{T-1}$ at 30.4382 induces a secondary kink in $\log(c) + \beta V_{T-1}(R(M - c) + y, 1)$ at $c = 18.4382$. In general we have that the secondary kink in c occurs at $c = M - (\overline{M}_{T-1} - y)/R$,

Figure 1: DC-EGM in period $T-2$ of the retirement problem, where $T=20$

(a) Multiple local optima near secondary kink

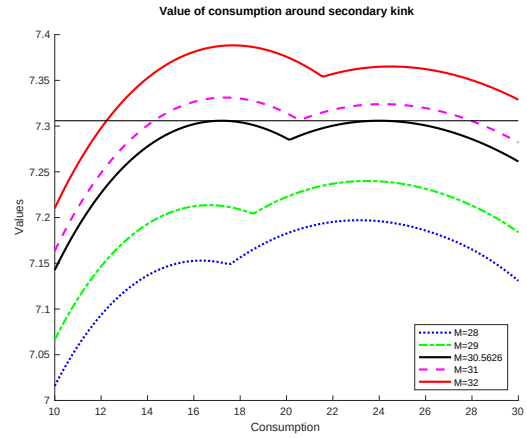

(b) Non-monotonic endogenous grid $\vec{M}$

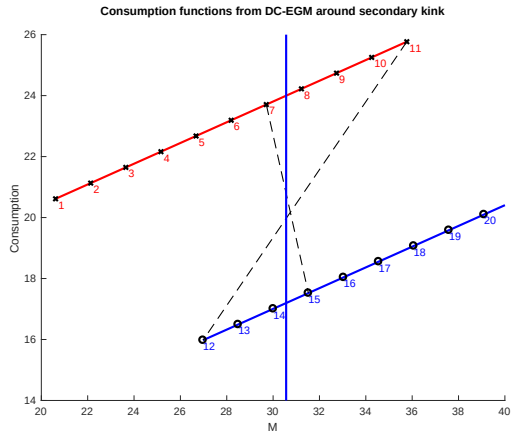

(c) Multiple solutions to Euler equations

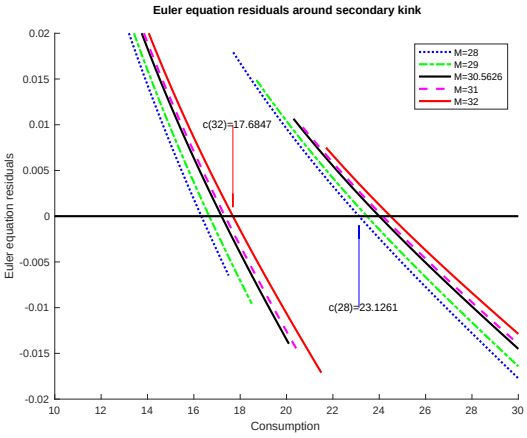

(d) Construction of the upper envelope

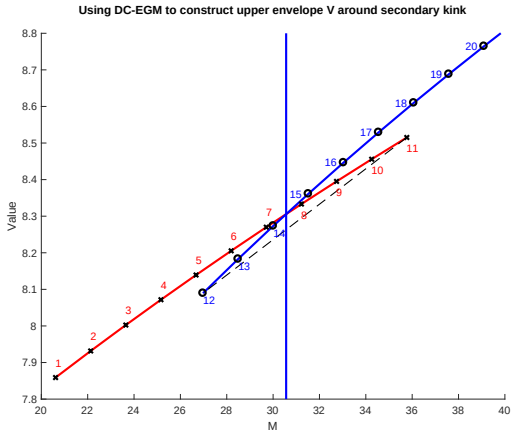

and thus increases monotonically in M.

The secondary kink in $\log(c)+\beta V_{T-1}(R(M-c)+y,1)$ leads to multiple locally optimal values of c on either side of the kink at $\overline{c}=M-(\overline{M}_{t-1}-y)/R$. Of course we are only interested in the *globally optimal solution* and from panel (a) we see that for $M<30.5626=\overline{M}_{T-2}^{r_1}$ (where the latter is the secondary kink where there is a discontinuous drop in consumption by Theorem 1) the global optimum is to the right of $\overline{c}$ whereas for $M>\overline{M}_{T-2}^{r_1}$ the global optimum is to the left of $\overline{c}$, and at $M=\overline{M}_{T-2}^{r_1}$ the consumer is indifferent between the two locally optimal solutions.

The multiplicity of locally optimal solutions for c in the region near the secondary kinks are also reflected in multiple solutions to the Euler equation for the worker (9) as you can see in panel (c)

of figure 1. There is also a discontinuity in the Euler residual function $u'(c) - \beta R u'(R(M-c)+y)$ at $c = \overline{c}$ caused by this secondary kink point. We now consider, how can the EGM method deal with Euler equations with discontinuities and multiple solutions? The short answer is that the standard EGM method cannot deal with these types of Euler equations, but we now show how, via the construction of the upper envelope of value functions, the DC-EGM algorithm we presented above does find the right solution.

Panel (b) of figure 1 shows the implied consumption function and endogenous grid $\vec{M}(1)$ that result from the application of the standard EGM method to solve the period $T-2$ Euler equation (9). We used an exogenous grid over savings equal to $\vec{A} = (0, 1, \ldots, 40)$ to construct the implied endogenous grid and consumption function using EGM. We plot the "solution" in panel (b), and label each of the points (M_j, c_j) resulting from the application of EGM to the first 20 exogenous saving grid points $A_1 = 0$, $A_2 = 1$, up to $A_{20} = 19$. The striking result is that EGM produces a *non-monotonic endogenous grid* $\vec{M}(1)$ as is indicated by the dotted line that connects $(M_{11}, c_{11}) = (35.76, 25.76)$ to the point $(M_{12}, c_{12}) = (26.97, 15.97)$. Of course this reflects both a discontinuity and drop in both M and c. Note also, EGM has produced a *consumption correspondence* rather than a *consumption function* because of the two possible consumption values at the endogenous grid points $(M_{12}, \ldots, M_{18})$. Which of the two consumptions is the correct one? In addition, the jump in this consumption correspondence at M_{11} going backward to an endogenous grid point $M_{12} < M_{11}$ creates a problem for standard EGM since we now show that a basic requirement for the correct solution is that the *endogenous grid must be monotonically increasing.*

To understand why this must be so, we define the *savings function* $A_t(M, d) = M - c_t(M, d)$ implied by the optimal consumption function $c_t(M, 1)$. Though Theorem 1 establishes that the consumption function can be discontinuous and *non-monotonic* we can establish the following Theorem under very weak conditions.

Theorem 2 (Monotonicity of the Saving Function)**.** *If u is strictly concave with monotone first derivative, then for each $t \in \{1, \ldots, T\}$ and each discrete choice $d \in \{0, 1\}$ the optimal saving function $A_t(M, d) = M - c_t(M, d)$ is monotone non-decreasing in M.*

The proof of Theorem 2 is in Appendix A. It implies that the non-monotonic endogenous grid $\vec{M}(1)$ illustrated in panel (b) of figure 1 is inconsistent with an optimal solution to the problem. How can this be rectified? In panel (d) of figure 1 we illustrate the key second step of DC-EGM — the construction of the upper envelope of the value functions. Thus, the value function interpolated

from the endogenous grid points $(M_1, \ldots, M_y)$ (indicated by the red line) is higher than the value function interpolated from endogenous grid points (M_{12}, M_{13}, M_{14}) (blue line). However at the vertical line at $\overline{M}_{T-2}^{r_1}$ the two interpolated functions cross, and for $M > \overline{M}_{T-2}^{r_1}$ the line marked with circular ordinates plots the value function interpolated from the endogenous grid points $(M_{15}, \ldots, M_{20})$ is higher than the line with ordinates are marked by x that plots the value function interpolated from endogenous grid points $(M_8, \ldots, M_{11})$. Thus, in the process of constructing the upper envelope, DC-EGM has identified *dominated endogenous grid points* $(M_8, \ldots, M_{14})$. If we eliminate these dominated endogenous grid points from the endogenous grid $\vec{M}(1)$, we obtain a new reduced endogenous grid $\vec{M}'(1) = \{M_1, \ldots, M_7, M_{15}, \ldots, M_{15}\}$ that is monotonic.

Using the reduced monotonic endogenous grid $\vec{M}'(1)$ constructed from the upper envelope of the interpolated value functions, we obtain a close approximation to the correct optimal consumption rule $c_{T-2}(M, 1)$ as we can see in panel (b) of figure 1. That is, for $M < \overline{M}_{T-2}^{r_1}$ optimal consumption is given by the upper line marked with x's, but for $M > \overline{M}_{T-2}^{r_1}$ optimal consumption is given by the lower line marked with cicles in panel (b) of figure 1. There is a discontinuous downward jump in consumption from endogenous grid point M_7 to the next point M_{15} on the reduced endogenous grid $\vec{M}'(1)$. As a further refinement, we can add an additional grid point to $\vec{A}'(1)$ equal to the point where the interpolated value functions cross in panel (d) of figure 1, which we can see is nearly equal to $\overline{M}_{T-2}^{r_1} = 30.4382$, the true secondary kink point of $V_{T-2}(M, 1)$ and point of discontinuity in $c_{T-2}(M, 1)$. Let's now call this modified endogenous grid $\vec{M}^*(1)$: it results from 1) a *dropping dominated points* from the original (non-monotonic) endogenous grid $\vec{M}(1)$, and 2) the addition of the kink point $\overline{M}_{T-2}^{r_1}$ where the two interpolated value functions cross. Using this modified, monotonic endogenous grid $\vec{M}^*(1)$, (even with small number of grid points J) DC-EGM produces very close approximations to the true solutions $V_{T-2}(M, 1)$ and $c_{T-2}(M, 1)$ that capture both the kink in V_{T-2} and the discontinuity in c_{T-2}.

This completes our description of DC-EGM: we can repeat the procedure above for all periods t to solve the retirement problem via backward induction on the Euler and Bellman equations. In the next section we verify that DC-EGM produces accurate approximations to $V_t(M, d)$, $c_t(M, d)$ and $d_t(M)$ at all periods $t \in \{1, \ldots, T\}$. It also generates accurate estimates of the secondary kink points $\overline{M}_t^{r_j}$ that capture discontinuous reductions in consumption that constitute saving for *anticipated retirement* that occur when a small increase in M *today* pushes the worker over a *future* retirement threshold.

2.3 Numerical performance of DC-EGM in the retirement problem

Figure 2 displays the optimal consumption function (6) and compares it to the numerical solution produced by DC-EGM described below in Section 3, as well as the numerical solution produced by a naive brute force implementation of value function iteration (VFI). VFI solves the Bellman equations (3) and (4) by backward induction over an *exogenous grid* on M and using numerical optimization to search for optimal consumption as each M grid point rather than attempting to compute optimal c from the Euler equations (9) and (10).[6] With a sufficient number of grid points, DC-EGM is able to accurately locate all the discontinuities of the analytical consumption rules ($\overline{M}_t^{r_j}$) and the boundary of the credit constrained region $y/R\beta$. Yet, because the kinks points $\overline{M}_t^{l_j}$ are not located precisely, the right panel of Figure 2 shows small relative errors on the order of 10^{-4} in the intervals $(y/R\beta, \overline{M}_{T-\tau}^{\tau-1})$ in each period $T-\tau$. Overall, the numerical solution by DC-EGM replicates the analytical solution remarkably well.[7]

Panels (c)-(d) of Figure 2 show the solution produced by VFI method with the same number of grid points over wealth and optimal consumption levels found by a fine grid search method. This implementation of VFI could admittedly be thought of as too simplistic, with possible improvements in how the grid points are located and spaced, which computational methods are employed to search for optimal consumption in each grid point, etc. Yet, the point we wish to make is that a standard "off the shelf" version of the VFI method may have serious difficulties when solving DC problems due to its failure to adequately capture the secondary kinks in the value function that get "papered over" via naive application of the standard method of linear interpolation of the value functions. The bottom panels of Figure 2 shows that the VFI solution results in significant approximation errors and is unable to fully capture the numerous discontinuities in the consumption function.

Figure 3 plots the optimal consumption functions and simulated consumption paths under the

[6] Simple linear interpolation of the value function ordinates at the exogenous gridpoints over M was used to implement numerical optimization for values of c where implied next period resources $R(M-c)+y$ does not line on the pre-defined exogenous grid $\vec{M}$. To enable a fair comparison with DC-EGM, we did use the *analytical solution* for the value function and consumption function of a retiree.

[7] With 2000 points on the endogenous grid over wealth it took our Matlab/C implementation around 0.17 seconds on a Lenovo ThinkPad laptop with Intel® Core™ i7-4600M CPU @ 2.10 GHz and 8GB RAM to generate the numerical solution by DC-EGM. This is about 20 times faster than VFI which we implemented in Matlab with 500 fixed grid points over wealth. The discretization of consumption is a brute force approach to ensure that global optimum is found. We used 400 equally spaced guesses for each level of wealth. The fact that EGM offers the speedup of one to two orders of magnitude relative to VFI is a well established finding in the literature, see e.g. Barillas and Fernández-Villaverde (2007); Jørgensen (2013); Fella (2014); Ameriks, Briggs, Caplin, Shapiro and Tonetti (2015).

Figure 2: Optimal Consumption Functions.

(a) Analytical Solution

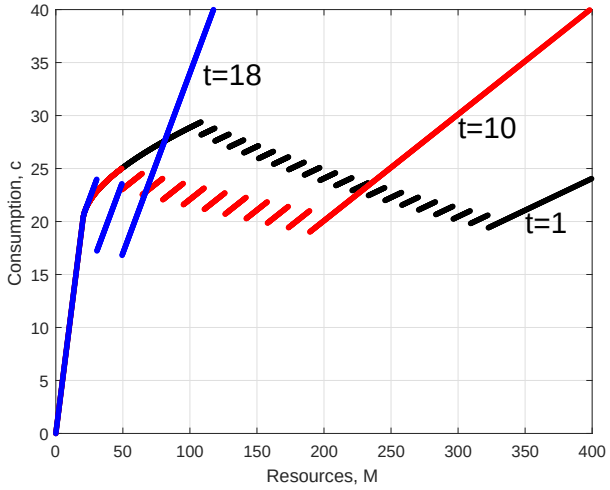

(b) Relative Error of DC-EGM solution

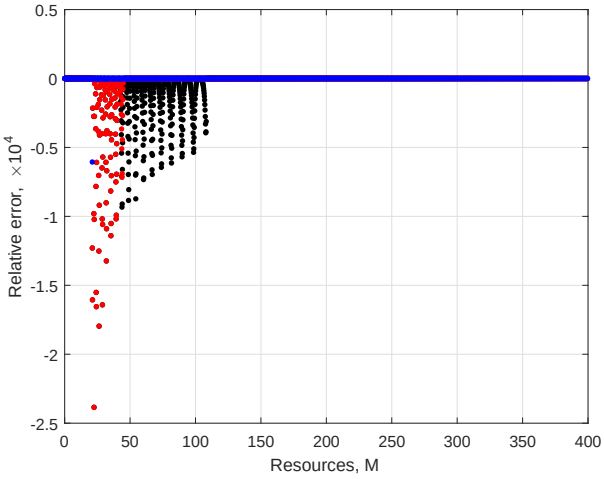

(c) Off the shelf VFI solution

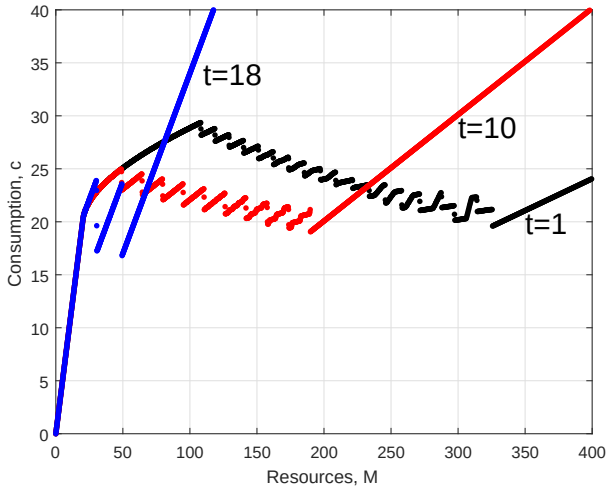

(d) Relative Error of VFI solution

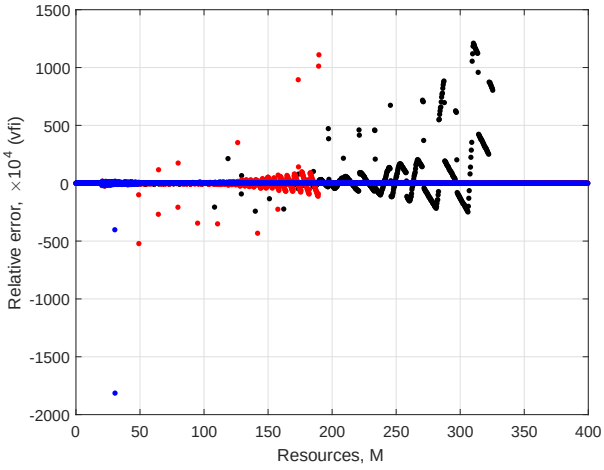

Notes: The plots show optimal consumption rules of the worker in the consumption-savings model with $R = 1$, $\beta = 0.98$, $y = 20$, and $T = 20$. Panel (a) illustrates the analytical solution (which is indistinguishable from the the numerical solution produced by DC-EGM), panel (b) illustrates the numerical error from the solution found by DC-EGM. Panel (c) shows the numerical solution found by VFI, and panel (d) shows the associated numerical errors. Both the VFI and DC-EGM solutions were generated using 2000 points in the M-grid. For VFI grid points are equally spaced, the maximum level in the wealth is 600, and 10,000 equally spaced between zero and $M(t)$ points of consumption are used to solve the maximization problem in the Bellman equation.

Figure 3: Discontinuous Consumption Function and Smooth Consumption Paths

(a) Consumption Function

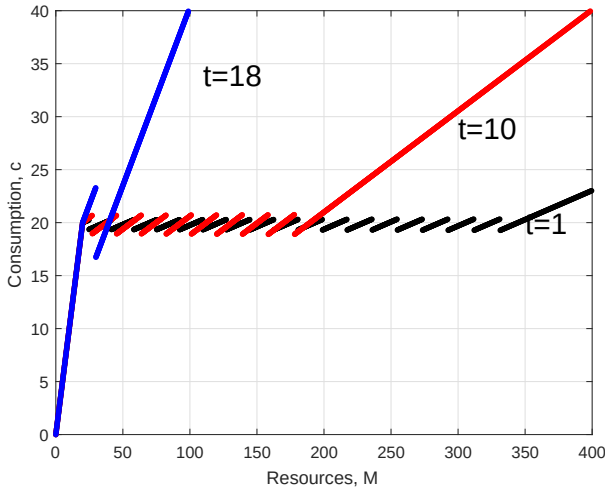

(b) Simulated Consumption Paths

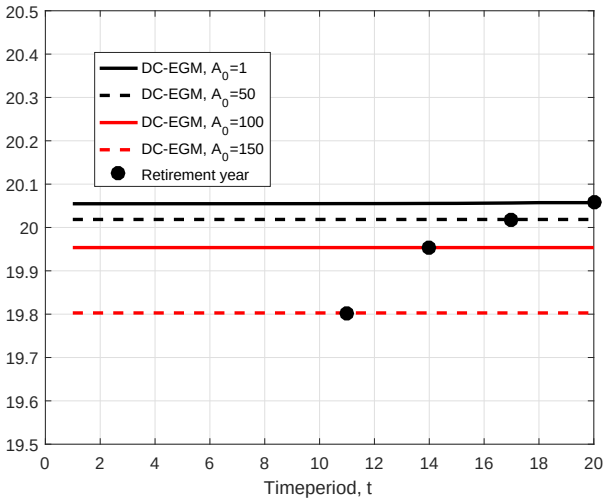

Notes: The plots show optimal consumption functions of the worker in the consumption-savings model with with $T = 20$, $d_t = 1$, $y = 20$, $\beta = .98$, and $R = 1/\beta = 1.02$. The left panel illustrates the solution for $t = 1, 10, 18$, while the right panel presents consumption paths simulated over the whole life cycle for several initial levels of wealth. The model was solved by the DC-EGM algorithm.

same assumptions as in Figure 2 except in this case we set $R = 1/\beta = 1.02$. The theoretical prediction is that, with $R\beta = 1$, simulated consumption paths should be flat, yet the consumption functions shown in the left panel displays numerous discontinuities that accumulate backwards from the final period $T = 20$. Beyond the important economic message that discontinuous consumption functions are not incompatible with consumption smoothing, this also illustrates the remarkable precision of the DC-EGM algorithm. In fact, when we simulate consumption trajectories implied by this incredibly complex solution found numerically, *the simulated consumption profiles are still perfectly flat.*

Before we describe in detail how DC-EGM works, we now illustrate how the incorporation of various types of uncertainty, including Extreme value taste shocks, renders the accumulation of kinks in the value function and discontinuities in the consumption function considerably less severe.

3 DC-EGM for problems with taste shocks

Now consider an extension of the model presented above where the consumer faces income uncertainty and where choices are affected by choice-specific taste shocks. More specifically, assume that income when working is $y_t = y\eta_t$, where η_t is log-normally distributed multiplicative idiosyncratic income shock, $\log \eta_t \sim \mathcal{N}(-\sigma_\eta^2/2, \sigma_\eta^2)$.[8]

The additively separable choice-specific random taste shocks, $\sigma_\varepsilon \varepsilon_t(d_t)$, are i.i.d. Extreme Value type I distributed with scale parameter σ_ε. In this formulation, the extreme value taste shock enters as a structural part of the problem. If the true model does not have taste shocks, σ_ε can be interpreted as a (logit) smoothing parameter, see Theorem 3 below.

The solution of the retiree's problem remains the same, and we focus on the worker's problem. The Bellman equation (2) has to be rewritten to include the taste shocks,

$$V_t(M, \varepsilon, 1) = \max\{v_t(M, 0) + \sigma_\varepsilon \varepsilon(0), v_t(M, 1) + \sigma_\varepsilon \varepsilon(1)\}, \tag{12}$$

where the value function conditional on the choice to retire $v_t(M, 0)$ is given by (3). However, the value function conditional on the choice to remain working, $v_t(M, 1)$, is modified to account for the taste and income shocks in the following period,

$$v_t(M, 1) = \max_{0 \le c \le M} \left\{ \log(c) - \delta + \beta \int EV_{t+1}^{\sigma_\varepsilon}(R(M - c) + y\eta, 1) f(d\eta) \right\}. \tag{13}$$

Because the taste shocks are independent Extreme Value distributed random variables, the expected value function, $EV_{t+1}^{\sigma_\varepsilon}$, is given by the well-known *logsum* formula (McFadden, 1973)

$$\begin{aligned} EV_{t+1}^{\sigma_\varepsilon}(M, 1) &= E\left[\max\left\{v_{t+1}(M, 0) + \sigma_\varepsilon \varepsilon(0),\ v_{t+1}(M, 1) + \sigma_\varepsilon \varepsilon(1)\right\}\right] \\ &= \sigma_\varepsilon \log\Big(\exp\{v_{t+1}(M, 0)/\sigma_\varepsilon\} + \exp\{v_{t+1}(M, 1)/\sigma_\varepsilon\}\Big). \end{aligned} \tag{14}$$

The immediate effect of introducing extreme value taste shocks is the complete elimination of the *primary* kinks due to the smoothing of the logit formula: the expected value function in (14) is a smooth function of M around the point where $v_t(M, 1) = v_t(M, 0)$. When σ_ε is sufficiently

[8] As mentioned above, we follow the literature in the assumption that idiosyncratic income shocks are realized *after* the labor supply choice is made, which is equivalent to allowing income to be dependent on a lagged choice of labor supply.

Figure 4: Optimal Consumption Rules for Agent Working Today ($d_{t-1} = 1$).

(a) Without income uncertainty, $\sigma_\eta = 0$

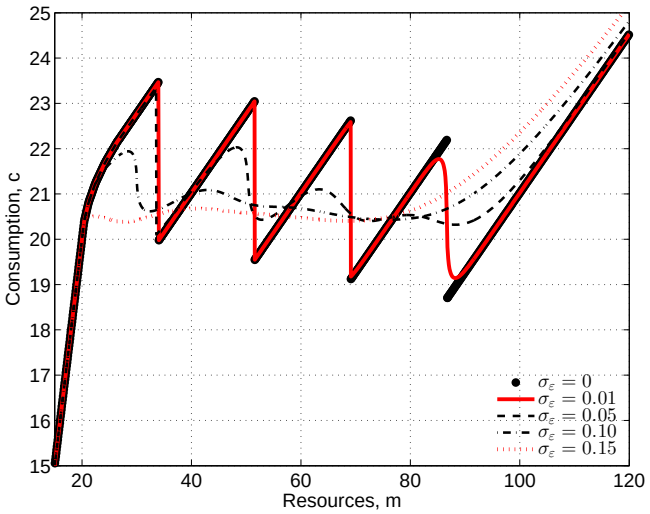

(b) With income uncertainty, $\sigma_\eta = \sqrt{.005}$

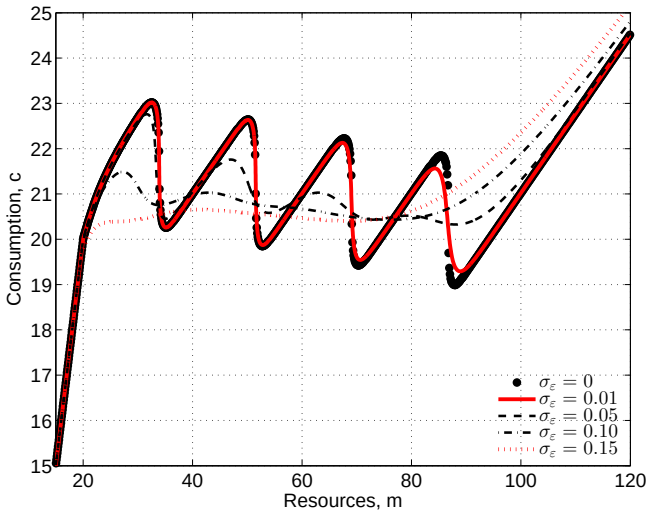

Notes: The plots show optimal consumption rules of the worker who decides to continue working in the consumption-savings model with retirement in period $t = T - 5$ for a set of taste shock scales σ_ε in the absence of income uncertainty, $\sigma_\eta = 0$, (left panel) and in presence of income uncertainty, $\sigma_\eta = \sqrt{.005}$, (right panel). The rest of the model parameters are $R = 1$, $delta = 1$, $\beta = 0.98$, $y = 20$.

large the value function $v_t(M, 1)$ eventually becomes globally concave.[9] Even when σ_ε is not large enough to "concavify" the value function completely, by smoothing out the primary kink in period t it still helps to eliminate many of the secondary kinks in the time periods prior to t.

Figure 4 shows the choice specific consumption function $c_t(M, 1)$ for a worker (conditional on the choice to continue working) for different values of smoothing parameter $\sigma_\varepsilon \in \{0, 0.01, 0.05, 0.10, 0.15\}$. The left panel plots the optimal consumption in the absence of income uncertainty ($\sigma_\eta = 0$) while income uncertainty ($\sigma_\eta = \sqrt{0.005}$) is added in the right panel. The plots are drawn for the period $T - 5$, corresponding to 4 discontinuities of the choice specific policy function in line with Theorem 1, without the discontinuity at the retirement threshold $\overline{M}_{T-5}$ in the deterministic model.

[9]To see this, note that as the variance of the taste shocks increases, the choice-specific value functions are dominated by the noise and the differences between the alternatives become relatively less important. In turn, the choice-specific value functions become similar, and $\lim_{\sigma_\varepsilon \downarrow \infty} EV_t^{\sigma_\varepsilon}(M)/\sigma_\varepsilon = log(2)$. It follows from (12) then that the value function $v_t(M, 1)$ inherits its globally concave shape from the utility function.

Figure 5: Artificial Discontinuities in Consumption Functions, $\sigma_\eta^2 = 0.01$, $t = T - 3$.

(a) $\sigma_\varepsilon = 0$ (b) $\sigma_\varepsilon = 0.05$

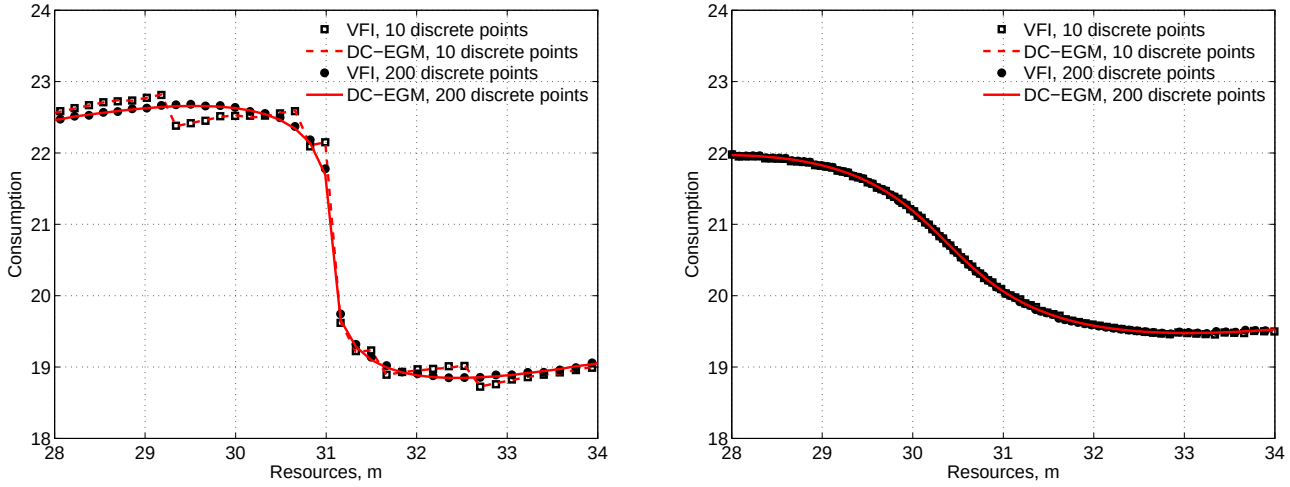

Notes: Figure 5 illustrates how the number of discrete points used to approximate expectations regarding future income affects the consumption functions from value function iteration (VFI) and DC-EGM. Panel (a) illustrates how using few (10) discrete equiprobable points to approximate expectations produce severe approximation error when there is *no* taste shocks. Panel (b) illustrates how moderate smoothing ($\sigma_\varepsilon = .05$) significantly reduces this approximation error.

It is evident that taste shocks of larger scale ($\sigma_\varepsilon \geq 0.05$) manage to smooth the function completely — eliminating all four discontinuities, and thus, eliminating the non-concavity of the value function in period $T-4$. Yet, for $\sigma_\varepsilon = 0.01$ only the last (rightmost) discontinuity is obviously smoothed out. Thus, even though full "concavification" is not achieved, the presence of extreme value taste shocks makes the consumption function continuous by smoothing out the secondary kinks in the value function.

When the model has other stochastic elements such as wage shocks or random market returns, the accumulation of secondary kinks may be less pronounced due to the additional smoothing. Yet, in the absence of taste shocks, the primary kinks cannot be avoided even if all secondary kinks are eliminated by a sufficiently high degree of uncertainty in the model. It is in this setup which also appears to be mostly used in practical applications, where the introduction of the Extreme Value distributed taste shocks is especially beneficial. The taste shocks *and* other structural shocks together contribute to the reduction of the number of secondary kinks and to the alleviation of the issue of their multiplication and accumulation. It is clear from the right panel of Figure 4 that the non-concavity of the value function can be eliminated with a smaller taste shock ($\sigma_\varepsilon = 0.01$)

when additional smoothing through uncertainty is present in the model.

An additional benefit of the inclusion of taste shocks is that numerical integration over the stochastic elements of the model has to be performed on a smooth function $EV_t^{\sigma_\varepsilon}(M,1)$ instead of the kinked value function $V_t(M,1)$. Standard procedures like Gaussian quadrature are readily applicable. When $\sigma_\varepsilon = 0$, performing standard numerical integration typically results in spurious discontinuities as shown in the left panel of Figure 5. This is due to the integrand not being a smooth function, see Appendix B for a detailed discussion. The right panel of Figure 5 illustrates how moderate smoothing ($\sigma_\varepsilon = .05$) significantly reduces this approximation error and removes the artificial kinks.

Thus, the extreme value taste shocks ε_t have a dual interpretation or role in DC models: in structural econometric applications, they can be regarded as unobserved state variables (i.e. variables observed by the consumer but not by the econometrician) that makes their behavior appear probabilistic from the standpoint of a person who does not observe ε_t. The shock ε_t also has an interpretation as stochastic noise that is introduced to help solve a difficult DC dynamic program by smoothing out kinks in the value function similar in some respects to the way stochastic noise is introduced into optimization algorithms to help them find a global optimum of difficult nonlinear programming problems with multiple local optima. In the former case, σ_ε is a scale parameter of taste shocks, and has to be estimated along with other structural parameters. In the latter case, σ_ε is the amount of smoothing and has to be chosen and fixed prior to estimation. Theorem 3 shows that the level of σ_ε can always be chosen in such a way that the perturbed model approximates the true deterministic model with an arbitrary degree of precision. In effect, Theorem 3 formalizes the results presented graphically in Figure 4.

Theorem 3 (Extreme Value Homotopy Principle)**.** *In every time period the (expected) value function of the consumption and retirement problem with extreme value taste shocks $EV_t^{\sigma_\varepsilon}(M_t)$ defined in* (14) *converges uniformly to the value function of the same problem without taste shocks $V_t(M,1)$ defined in* (2) *as the scale of these shocks approaches zero. The following uniform bound holds*

$$\forall t: \quad \sup_{M\geq 0} |EV_t^{\sigma_\varepsilon}(M,1) - V_t(M,1)| \leq \sigma_\varepsilon \left[\sum_{j=0}^{T-t} \beta^j\right] \log(2). \tag{15}$$

Consequently, as $\sigma_\varepsilon \downarrow 0$, both continuous and discrete decision rules of the smoothed model with taste shocks converge pointwise to those of the deterministic model.

In Appendix E we prove a more general version of Theorem 3 which holds under very weak conditions for arbitrary DC models with multidimensional continuous or discrete state variables and multiple continuous choice variables. Theorem 3 justifies our claim that the extreme value smoothing can be regarded as a homotopy method for solving the non-smooth limiting problem without taste shocks by solving a smooth "nearby" problem with Extreme value taste shocks. The Extreme value scale parameter σ_ε plays the role of the "homotopy parameter."

3.1 Extending DC-EGM for Taste Shocks and Income Uncertainty

The DC-EGM algorithm remains the same for problems with taste shocks and income uncertainty, though the Euler equation that is recursively solved changes to the version given below

$$\begin{aligned} 0 &= u'(c) - \beta R \int [u'(c_{t+1}(R(M-c)+y\eta,1)P_{t+1}(1|R(M-c)+y\eta)+ \\ &\quad u'(c_{t+1}(R(M-c),0)P_{t+1}(0|R(M-c)+y\eta)]\, f(d\eta), \end{aligned} \tag{16}$$

where $P_t(1|M)$ and $P_t(0|M)$ are *conditional choice probabilities* given by the *binomial logit formula* of McFadden (1973)

$$\begin{aligned} P_t(1|M) &= \frac{\exp\{v_t(M,1)/\sigma_\varepsilon\}}{\exp\{v_t(M,1)/\sigma_\varepsilon\} + \exp\{v_t(M,0)/\sigma_\varepsilon\}} \\ P_t(0|M) &= \frac{\exp\{v_t(M,0)/\sigma_\varepsilon\}}{\exp\{v_t(M,1)/\sigma_\varepsilon\} + \exp\{v_t(M,0)/\sigma_\varepsilon\}}. \end{aligned} \tag{17}$$

If we continue to assume that retirement is an absorbing state, the optimal consumption rule for a retiree, $c_t(M,0)$ can be calculated using the standard EGM algorithm as described in section 2.2. It is also possible to allow for stochastic returns on savings, $\tilde{R}$ and this just requires an additional integration on the right hand side of the Euler equation (16) to compute the expectation of period $t+1$ marginal utility over the distribution of returns.

Given $c_t(M,0)$, we then solve (16) via the same backward induction process as described in section 2.2 for the retirement problem without stochastic shocks, starting with the easily derived result that $C_T(M,1) = M$ and $d_T(M) = 0$ (i.e. it is always optimal to retire and consume all remaining wealth in the last period of life). Then working backward, we choose an exogenous grid over saving $\vec{A} = (A_1, \ldots, A_J)$ (which remains fixed throughout the backward induction process) and compute optimal consumption $\{c_t(A_1,1), \ldots, c_t(A_J,1)\}$ for each point A_j in the exogenous

grid over saving by analytically inverting marginal utility as follows

$$c_t(A_j, 1) = \tag{18}$$
$$u'^{-1}\left(\beta R \int \left[u'(c_{t+1}(RA_j + y\eta, 1))P_{t+1}(1|RA_j + y\eta) + u'(c_{t+1}(RA_j, 0))P_{t+1}(0|RA_j)\right] f(d\eta)\right).$$

Using these consumptions, we construct the endogenous grid over M as $\vec{M}_t(1) = (M_{t,1}, \ldots, M_{t,J})$ where M_j is given by

$$M_{j,t} = c_t(A_j, 1) + A_j, \quad j \in \{1, \ldots, J\}. \tag{19}$$

If the resulting gridpoints are a montonically increasing sequence, then no violation of monotonicity of the saving function as per Theorem 2 is indicated, and the DC-EGM method automatically reverts to the standard EGM method of Carroll (2006). However if $\vec{M}_t(1)$ is not a monotonically increasing sequence, we apply the upper envlope procedure as described in section 2.2 to eliminate the dominated elements of $\vec{M}_t(1)$ and add a point corresponding to the kink point where the disjoint segments of the value function intersect. We then use the resulting modified, monotonic endogenous grid $\vec{M}^*_t(1)$ to calculate (via interpolation) the upper envelope leading to $v_t(M, 1)$ and the implied consumption function for a worker, $c_t(M, 1)$. We continue this procedure from period $T - 1$ backward to period $t = 1$, at which point we have fully approximated the solution to the life cycle retirement problem by DC-EGM.

Algorithm 1 provides pseudo-code for the first part of DC-EGM which we call *the EGM step*. The current period discrete choice, d_t, and the next period policy and value functions are inputs to this routine, while the endogenous grid $\vec{M}_t = M_t(\vec{A}, d)$ and the d-specific consumption and value functions, $c_t(\vec{M}_t, d) = c_t(\vec{A}, d)$ and $v_t\big(\vec{M}_t, d\big) = v_t\big(M_t(\vec{A}), d\big)$ computed on this grid are the outputs.

Figure 6 plots a selection of values of $v_t\big(\vec{M}_t, 1\big)$ and $c_t(\vec{M}_t, 1)$ against the endogenous grid $\vec{M}_t$. The points are indexed in the ascending order of the end-of-period wealth forming the grid $\vec{A}$. The solid lines approximate the corresponding functions with linear interpolation. It is evident that, similar to the case without taste shocks in section 2.2, the interpolated choice-specific value function $v_t\big(M, 1\big)$ is a *correspondence rather than a function* because of the existence of the region where multiple values of $v_t\big(M|d_t\big)$ correspond to a single value of M. The same is true for the interpolated choice-specific consumption function. Adding taste shocks with a relatively low variance, $\sigma_\varepsilon = 0.03$, reduces the size of the regions with multiple corresponding values but does not eliminate it. Dashed

Algorithm 1 The EGM-step: choice-specific consumption and value functions

1: **Inputs:** Current decision d_t. Choice-specific consumption and value functions $c_{t+1}(\vec{M}_{t+1}, d)$ and $v_{t+1}(\vec{M}_{t+1}, d)$ associated with the endogenous grid in period $t+1$, $\vec{M}_{t+1}(d)$
2: Let $\vec{\eta} = \{\eta_1, \ldots, \eta_Q\}$ be a vector of quadrature points with associated weights, $\vec{\omega} = \{\omega^1, \ldots, \omega^Q\}$
3: Form an ascending grid over end-of-period wealth, $\vec{A} = \{A_1, \ldots, A_J\}$ where $A^j > A^{j-1}$, $\forall j \in \{2, \ldots, J\}$
4: **for** $j = 1, \ldots, J$ **do** (Loop over points in $\vec{A}$)
5: **for** $q = 1, \ldots, Q$ **do** (Loop over quadrature points in $\vec{\eta}$)
6: Compute $M^q_{t+1}(A_j) = RA_j + dy\eta_q$
7: **for** $d = 0, 1$ **do**
8: Compute $c_{t+1}(M^q_{t+1}(A_j), d)$ by interpolating $c_{t+1}(\vec{M}_{t+1}, d)$ at the point $M^q_{t+1}(A_j)$
9: Compute $v_{t+1}\big(M^q_{t+1}(A_j)|d\big)$ by interpolating $v_{t+1}(\vec{M}_{t+1}|d)$ at the point $M^q_{t+1}(A_j)$
10: **end for**
11: Compute $\phi_{t+1}\big(M^q_{t+1}(A_j)\big) = \sigma_\varepsilon \log\big(\sum_{d=0,1} \exp(v_{t+1}\big(M^q_{t+1}(A_j), d\big)/\sigma_\varepsilon\big)$
12: Compute $P_{t+1}(d|M^q_{t+1}(A_j)) = \exp(v_{t+1}\big(M^q_{t+1}(A_j), d\big)/\sigma_\varepsilon)(\sum_{d=0,1} \exp(v_{t+1}\big(M^q_{t+1}(A_j)|d\big))/\sigma_\varepsilon)^{-1}$
13: **end for**
14: Compute $\text{RHS}\big(M_{t+1}(A_j)\big) = \beta R \sum_{q=1}^{Q} \sum_{d=0,1} \omega^q \cdot u'\big(c_{t+1}(M^q_{t+1}(A_j)|d)\big) \cdot P_{t+1}(d|M^q_{t+1}(A_j))$
15: Compute expected value function $EV_{t+1}\big(M_{t+1}(A_j, d)\big) = \sum_{q=1}^{Q} \omega^q \cdot \phi_{t+1}\big(M^q_{t+1}(A_j)\big)$
16: Compute current consumption $c_t(A_j|d) = u'^{-1}\Big(\text{RHS}\big(M_{t+1}(A_j)\big)\Big)$
17: Compute value function $v_t\big(M_t(A^j), d\big) = u(c_t(A_j, d)) + \beta EV_{t+1}\big(A_j, d\big)$
18: Compute endogenous grid point $M_t(A_j, d) = c_t(A_j, d) + A_j$
19: **end for**
20: Collect the points $M_t(A_j, d)$ from the endogenous grid $\vec{M}_t = \{M_t(A_j, d), j = 1, \ldots, J\}$ associated with the choice-specific consumption and value functions: $c_t\big(\vec{M}_t, d\big) = \{c_t\big(M_t(A_j), d\big), j = 1, \ldots, J\}$, and $v_t\big(\vec{M}_t, d\big) = \{v_t\big(M_t(A_j), d\big), j = 1, \ldots, J\}$
21: **Outputs:** $\vec{M}_t(d)$, $c_t(\vec{M}_t(d), d)$ and $v_t\big(\vec{M}_t(d), d\big)$

Notes: The pseudo code is written under the assumption that quadrature rules are used for calculating the expectations, whereas particular implementations can employ other methods for computing the expectation. It is also assumed that interpolation rather than approximation is used in Steps 8 and 9, although the latter is also possible.

lines illustrate discontinuities.

The region where multiple values of $v_t\big(M, 1\big)$ correspond to a single value of M is the clear evidence of non-concavity of the value function in the following period, and subsequent multiplicity of solutions of the Euler equation. We should emphasize, however, that the points produced by the EGM step necessarily contain the true solutions. This is a notable contrast to the standard solution methods based on an exogenous grid over wealth, which may struggle to find the points of optimality and have to deploy computationally costly global search methods to solve the optimization problem in the Bellman equation.

The next section describes a procedure in DC-EGM algorithm that deals with selecting the true optimal points among the points produced by the EGM step. The true solution found by the full DC-EGM algorithm is illustrated in Figure 6 with a red line for reference.

Figure 6: Non-concave regions and the elimination of the secondary kinks in DC-EGM.

(a) Upper Envelope

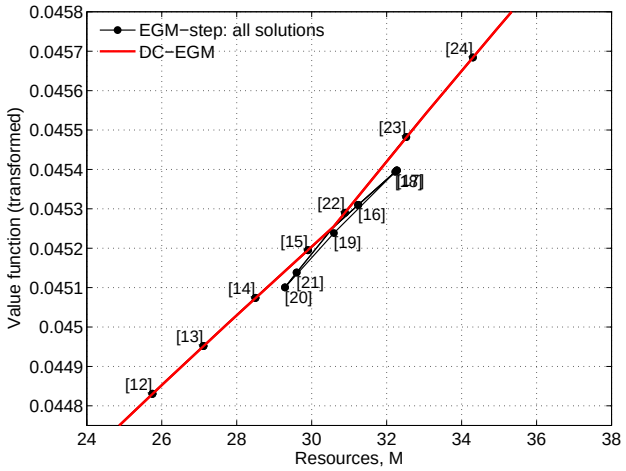

(b) Implied Consumption

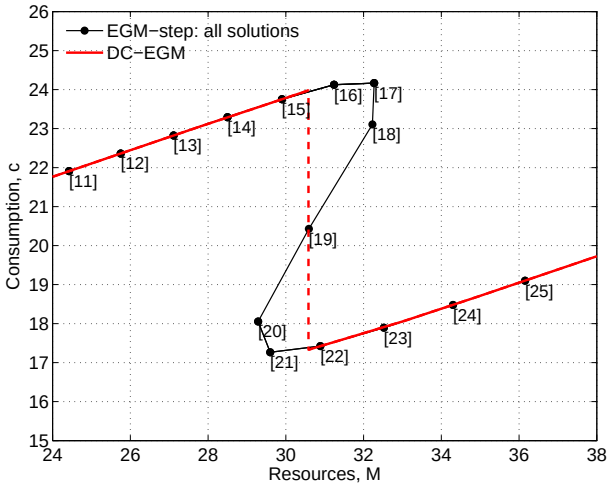

Notes: The plots illustrate the output from the EGM-step of the DC-EGM algorithm (Algorithm 1) in a non-concave region. The dots are indexed with the index j of the exogenous grid over saving $\vec{A} = \{A_1, \ldots, A_J\}$ where $A_j > A_{j-1}$, $\forall j \in \{2, \ldots, J\}$. The connecting lines show the d-specific value functions $v_t(\vec{M}_t|d)$ and the consumption function $c_t(\vec{M}_t|d)$ linearly interpolated on the endogenous grid $\vec{M}_t$. The left panels illustrates construction of the upper envelope from which $v_t(\vec{M}_t|d)$ is interpolated. The "true" solution, after applying the DC-EGM algorithm is illustrated with a thick solid red line. Dashed lines illustrate discontinuities. The solution is based on $G = 70$ grid points in $\vec{A}_t$, $R = 1$, $\delta = 1$. $\beta = 0.98$, $y = 20$, $\sigma_\eta = 0$, and $\sigma_\varepsilon = 0.03$.

3.2 Calculation of the Upper Envelope

To distinguish between the optimal and suboptimal points produced by the EGM step, the DC-EGM algorithm makes a direct comparison of the values associated with each of the choices. On the plots of the choice-specific value function correspondences in Figure 6, this amounts to computing the *upper envelope* of the correspondence in the regions of M where multiple solutions are found.

We conclude that even in the presence of taste shocks, the problem of multiplicity of local maxima in the maximand of equation (13) is generally still present. This implies that there still can be discontinuities consumption. In other words, the taste shocks may not fully "concavify" the value function. Note that in the smooth case there can be three solutions to the Euler equation, only one of which is a global maximum. However just as in the case without taste shocks that we illustrated in section 2.2, we can identify the correct (i.e. globally optimal) soltuion the Euler equation in the process of constructing the upper envelope $v_t(M, 1)$.

It is clear, that selecting the global maximum among the critical points located by solving the Euler equation during the EGM step amounts to comparing the values of the constructed value function correspondence $v_t(M_t(d), d)$ for each $M_t(d)$. For comparison, the overlapping segments of $v_t(M_t(d), d)$ may have to be re-interpolated on some common grid, and the upper envelope has to be computed. Algorithm 2 presents the pseudo-code of this calculation. The key insight of the upper envelope algorithm is to use the monotonicity of the end-of-period resources as a function of wealth to detect the regions where multiple values of choice-specific value function $v_t(M_t(d), d)$ are returned for a single value of $M_t(d)$ (see Step 3 of Algorithm 2). Monotonicity of end-of-period wealth is due to the concavity of the utility function as shown in Theorem 2, see Appendix A. Around every such detected region, the value function correspondence is broken into three segments (Steps 5 to 7), which are then compared point-wise to compute the upper envelope (Step 12). The inferior points are simply dropped from the endogenous grid $\vec{M}_t(d)$, and optionally the approximated kink points at the inserted. Consequently, the consumption and value function correspondences are cleaned up and become *functions*.

While the DC-EGM is similar to the approach proposed in Fella (2014), we explicitly allow for extreme value type I taste shocks to preferences and show how they help with the computational issues specific to the model of discrete-continuous choices. The approach in Fella (2014) does not readily apply to the class of models with taste shocks but should be adjusted along the lines described here. Particularly, the DC-EGM operates with discrete choice specific value functions

Algorithm 2 Upper envelope refinement step

1: **Inputs:** Endogenous grid $\vec{M}_t(d) = M_t(\vec{A}, d)$ obtained from the grid over the end-of-period resources $\vec{A}_t = \{A_1, \ldots, A_J\}$ where $A_j > A_{j-1}$, $\forall j \in \{2, \ldots, J\}$; saving and value function *correspondences* $c_t(\vec{M}_t(d), d)$ and $v_t\big(\vec{M}_t(d), d\big)$ computed on $\vec{M}_t(d)$
2: **for** $j = 2, \ldots, J$ **do** (Loop over the points of endogenous grid)
3: **if** $M_t(A_j) < M_t(A_{j-1})$ **then** (Criterion for detecting non-concave regions)
4: Find the first $h \geq j$ such that $M_t(A_h, d) < M_t(A_{h+1}, d)$
5: Let $J_1 = \{j' : j' \leq j - 1\}$ (Points up to [19] in panel a and [17] in panel b of Figure 6)
6: Let $J_2 = \{j' : j - 1 \leq j' \leq h\}$ (Points [19], [20] in panel a and [17]-[20] in panel b of Figure 6)
7: Let $J_3 = \{j' : h \leq j'\}$ (Points [20] and up in both panel a and b of Figure 6)
8: Let $\vec{M}' = \{M_t(A_{j'}) : \min_{i \in J_2} M_t(A_i) = M_t(A_h) \leq M_t(A_{j'}) \leq M_t(A_{j-1}) = \max_{i \in J_2} M_t(A_i)\}$
9: **for** $i = 1, \ldots, |\vec{M}'|$ **do** where $|\vec{M}'|$ is the number of points in $\vec{M}'$
10: Denote $v_t\big(\vec{M}_t(d), d, J_r\big)$ the segment of $v_t\big(\vec{M}_t(d), d\big)$ computed on the points in the set J_r
11: Interpolate the segments $v_t\big(\vec{M}_t(d), d, J_r\big)$ at the point $M_t(A_i)$ if $i \notin J^r$, $r = 1, \ldots, 3$
12: **if** $v_t\big(M_t(A_i, d), d\big) < \max_r v_t\big(M_t(A_i, d), d, J^r\big)$ **then**
13: Drop point i from the endogenous grid $\vec{M}_t(d)$
14: **end if**
15: **end for**
16: Find the point $M^* : v_t\big(M^*, d, J^3\big) = v_t\big(M^*, d, J^1\big)$ [Optional]
17: Insert M^* into $\vec{M}_t(d)$ first with associated values $v_t\big(M^*|d, J^3\big)$ and $c_t\big(M^*|d, J^3\big)$ [Optional]
18: Insert M^* into $\vec{M}_t(d)$ then with associated values $v_t\big(M^*(d), d, J^1\big)$ and $c_t\big(M^*(d), d, J^1\big)$ [Optional]
19: Set $j = h$
20: **else**
21: Keep point j on the endogenous grid $\vec{M}_t(d)$ as is
22: **end if**
23: **end for**
24: **Outputs:** Refined endogenous grid $\vec{M}_t(d)$, consumption and value *functions* $c_t(\vec{M}_t(d), d)$ and $v_t\big(\vec{M}_t(d), d\big)$

Note: The pseudo code is written using an elementary algorithm for calculation of the upper envelope for a collection of functions defined on their individual grids. More efficient implementations could also be used, see for example (Hershberger, 1989). Inserting the intersection point into the endogenous grid $\vec{M}_t(d)$ *two times* in step 17 and 18 ensures an accurate representation of the discontinuity in consumption function $c_t(\vec{M}_t(d), d)$. If the optional steps 16-18 are skipped, the secondary kink is smoothed out, but the overall shapes of the consumption and value functions are correct.

and optimal consumption rules, and computes integrals of smooth objects. Furthermore, contrary to Fella (2014) who uses instances of increasing marginal utility to detect non-concave regions, DC-EGM uses the value function correspondence. However, both approaches rely on monotonicity of the optimal end-of-period savings function.

Algorithm 3 presents the pseudo-code of the full DC-EGM algorithm, which invokes the EGM step (Algorithm 1) repeatedly to compute the value function correspondences for all discrete choices, and then finds and removes all suboptimal points on the returned endogenous grids by calling the upper envelope module (Algorithm 2).

An important question of how the method handles the situations when the non-convex regions

Algorithm 3 The DC-EGM algorithm

1: In the terminal period T fix a grid $\vec{M}_T$ over the consumable wealth M_T. On this grid compute consumption rules $c_T(\vec{M}_T(d), d) = \vec{M}_T$ and value functions $v_T(\vec{M}_T, 0) = (\log(\vec{M}_T))$ for $d = 0$. This provides the base for backward induction in time
2: **for** $t = T-1, \ldots, 1$ **do** (Loop backwards over the time periods)
3: **for** $d = \{0, 1\}$ **do** (Loop over the current period discrete choices)
4: Invoke the EGM step (Algorithm 1) for choice d, $c_{t+1}(\vec{M}_{t+1}(d), d)$ and $v_{t+1}(\vec{M}_{t+1}(d), d)$ as inputs
5: Invoke upper envelope (Algorithm 2) using outputs from Step 4, $\vec{M}_t(d)$, $c_t(\vec{M}_t(d), d)$ and $v_t\big(\vec{M}_t(d), d\big)$ as inputs
6: The endogenous grid $\vec{M}_t(d)$ and consumption and value functions $c_t(\vec{M}_t(d), d)$ and $v_t\big(\vec{M}_t(d), d\big)$ are now computed
7: **end for**
8: **end for**
9: The collection of the choice-specific consumption and value functions $c_t(\vec{M}_t(d), d)$ and $v_t(\vec{M}_t(d), d)$ defined on the endogenous grids $\vec{M}_t(d)$ for $d = \{0, 1\}$ and $t = \{1, \ldots, T\}$ constitutes the solution of the consumption/savings and retirement model

go undetected due to relatively coarse grid $\vec{A}$ is addressed by the Monte Carlo simulations in the next section. We show that even with small number of endogenous grid points the Nested Fixed Point (NFXP) Maximum Likelihood estimator based on the DC-EGM algorithm performs well and is able to identify the structural parameters of the model.

3.3 Credit Constraints

Before turning to the Monte Carlo results, we briefly discuss how DC-EGM handles the credit constraints, $c \leq M$. During the EGM step, the credit constraints are dealt with in exactly same manner as in Carroll (2006). Let the smallest possible end-of-period resources $A_1 = 0$ be the first point in the exogenous grid over saving $\vec{A}$. Assuming that the corresponding point of the endogenous grid $M_t(A_1, d)$ is positive[10], it holds that $A(M, d) = 0$ for all $M \leq M_t(A_1, d)$ due to the monotonicity of saving function $A(M, d) = M - c_t(M, d)$ (see Theorem 2). Therefore, the optimal consumption in this region is then given by $c_t(M, d) = M$, and the choice-specific value function is

$$v_t(M, d) = \log(M) - d\delta_t + \beta \int EV_{t+1}(dy\eta) f(d\eta), \quad M \leq M_t(A_1, d). \tag{20}$$

Note that the third component of (20) is the expected value of having zero savings. It is calculated within the EGM step for the point $A_1 = 0$, and should be saved separately as a constant that depends on d but not on M. Once this constant is computed, $v_t(M, d)$ essentially has analytical form in the interval $[0, M_t(A_1, d)]$, and thus can be directly evaluated at any point.

[10]It is not hard to show that this holds as long as the per period utility function satisfies the Inada conditions.

When the per-period utility function is additively separable in consumption and discrete choice like in the retirement model we consider, (20) holds for all $d \in D_t$ in the interval $0 \leq M \leq \min_{d \in D_t} M_t(A_1, d)$. In other words, the choice specific value functions for low wealth have the same shape (in our case $\log(M)$), which is shifted vertically with d_t-specific coefficients. This implies that the logistic choice probabilities $P_t(d|M)$ are constant in this interval, and have to only be calculated once.

4 Monte Carlo Results

In this section we investigate the properties of the *approximate* maximum likelihood estimator (MLE) that we obtain using the DC-EGM to approximate the model solution in the inner loop of the Nested Fixed Point algorithm. We specifically focus on role of income uncertainty and taste shocks for the approximation bias induced by a numerical solution with a finite number of grid-points; in particular how approximation bias depends on the number of grid points in smooth as well as non-smooth problems. After a description of the data generating process (DGP), we present the results from a series of Monte Carlo experiments, and show that models used in typical empirical applications are sufficiently smooth to almost eliminate approximation bias using relatively few grid points.

4.1 Data Generation Process

For the Monte Carlo we consider a slightly more general formulation of the consumption/savings and retirement problem defined in (1) with constant relative risk aversion (CRRA) utility

$$\max_{\{c_t, d_t\}_1^T} \sum_{t=1}^{T} \beta^t \left(\frac{c_t^{1-\rho} - 1}{1-\rho} - \delta_t d_t \right) \tag{21}$$

where ρ is the CRRA coefficient.

In order to simulate synthetic data from the DGP consistent with the model and the vector of *true* parameter values, we solve the model *very accurately* with 2,000 grid points using the DC-EGM. We refer to this solution as the *true solution* even though this is off course only an accurate finite approximation of the value function.[11]

[11] As a spot check, we have also compared this solution with the traditional value function iteration approach, where we used a grid search over 1,000 discrete points on the interval $[0, M_t]$ to locate the optimal consumption for

Table 1: Baseline *true* parameter values.

Description	Value	Description	Value
Time horizon	$T = 44$	Disutility of work	$\delta = 0.5$
Gross interest rate	$R = 1.03$	Discount factor	$\beta = 0.97$
Full time employment income	$y = 1.0$	CRRA coefficient	$\rho = 2.0$
Income variance	$\sigma_\eta = 0$	Taste shocks scale	$\sigma_\varepsilon \in \{0.01, 0.05\}$

We consider several specifications of the model in the Monte Carlo experiments below to study various aspects of the performance of the estimator. Once again, we assume that disutility of work is constant over time, i.e. $\delta_t = \delta$. Table 1 presents the parameter values in the baseline specification of the model. Deviations are given explicitly with every Monte Carlo experiment separately. We perform 200 replications for each combination of settings.

For each specification of the model, 50,000 individuals are simulated for $T = 44$ periods. Each individual i is initiated as full-time worker $s^d_{i,1} = 1$, where we have used $s^d_{i,t} \in \{0, 1\}$ to denote the labor market state, i.e. whether an individual is retired ($s^d_{i,t} = 0$) or working ($s^d_{i,t} = 1$). Each workers initial wealth $M^d_{i,1}$ is drawn from a uniform distribution on the interval $[0, 100]$. At the beginning of each time period t, a random log-normal labor market income shock η_t with variance parameter σ_η is drawn if the individual i is working and individual's resources M^d_t are calculated. Given the level of resources, discrete-choice specific value functions and choice probabilities are computed, and a random draw determines which discrete labor market option d^d_{it} is chosen. After one period lag, the labor force participation decision becomes the labor market state, $s^d_{i,t+1} = d^d_{it}$. The optimal level of consumption, c_{it}, is then computed conditional on d^d_{it}, and the end-of-period wealth is calculated and stored to be used for calculation of resources available in the beginning of period $t + 1$, $M^d_{i,t+1}$. We then add normal additive measurement error with standard deviation $\sigma_\xi = 1$ to get the simulated consumption data, c^d_{it}. This produces simulated panel data $(M^d_{it}, s^d_{it}, d^d_{it}, c^d_{it})$ for each individual $i \in \{1, \ldots, 50, 000\}$ in all time periods $t \in \{1, \ldots, 44\}$.

4.2 Maximum Likelihood Estimation

We implement a discrete-continuous version of the Nested Fixed Point (NFXP) Maximum Likelihood estimator devised in Rust (1987, 1988), where we augment the original discrete-choice estimator with a measurement error approach when assessing the likelihood of the observed continuous

each value of wealth. We find that results are essentially identical.

choices.

Assume that a panel dataset is available, $\{(M_{it}^d, s_{it}^d, d_{it}^d, c_{it}^d)\}_{i=\{1,\ldots,N\},\, t=\{1,\ldots,T\}}$, containing observations on wealth, labor market state, discrete and continuous choices of individuals $i = 1 \ldots, N$ in time periods $t = 1, \ldots, T$. Let $c_t(M_t, s_t, d_t|\theta)$ denote the consumption policy function computed by the DC-EGM for a given vector of model parameters $\theta = (\delta, \beta, \rho, \sigma_\eta, \sigma_\varepsilon)$. We assume that consumption is observed with additive Gaussian measurement error,

$$c_{it}^d = c_t(M_{it}^d, s_{it}^d, d_{it}^d|\theta) + \xi_{it},\ \xi_{it} \sim N(0, \sigma_\xi),\ \text{i.i.d. } \forall i, t. \tag{22}$$

Let $\xi_{it}^d(\theta) = c_{it}^d - c_t(M_{it}^d, s_{it}^d, d_{it}^d|\theta)$ denote the difference between the predicted and the observed consumption. We assume that the measurement error, ξ_{it}, is independent of the taste shocks, $\varepsilon_t(d_t)$, and, thus, the joint likelihood of observation i in period t is given by

$$\ell_{it}(\theta, \sigma_\xi) = P(d_{it}^d|M_{it}^d, s_{it}^d, \theta)\frac{\phi(\xi_{it}^d(\theta)/\sigma_\xi)}{\sigma_\xi}, \tag{23}$$

where $\phi(\cdot)$ is the density function of the standard normal distribution. We have ignored the controlled transition probability for the retirement status s_{it}^d, since $P_{tr}(s_{it}^d|s_{i,t-1}^d, d_{i,t-1}^d)$ is always 1 in the data when retirement is absorbing and the labor market state is perfectly controlled by the decision.

The choice probabilities for the workers ($s_{it}^d = 1$) are standard logits

$$P(d_{it}^d|M_{it}^d, s_{it}^d, \theta) = \frac{\exp(v_t(M_{it}^d, s_{it}^d, d_{it}^d|\theta)/\sigma_\varepsilon)}{\sum_{j=0}^1 \exp(v_t(M_{it}^d, s_{it}^d, j|\theta)/\sigma_\varepsilon)} \tag{24}$$

and are computed from the discrete choice specific value functions $v_t(M_{it}^d, s_{it}^d, d_{it}^d|\theta)$ found by the DC-EGM given a particular value of the parameter vector θ, evaluated at the data. Because retirement is absorbing and thus retirees do not have any discrete choice to make, the first component of individual likelihood contribution (23) drops out when $s_{it}^d = 0$.

The joint log-likelihood function is given by $\tilde{\mathcal{L}}(\theta, \sigma_\xi) = \log \prod_i^N \prod_t^T \ell_{it}(\theta, \sigma_\xi)$ where re-arranging the first order condition with respect to σ_ξ^2 yields the standard ML estimator for the measurement error variance, $\sigma_\xi^2(\theta) = \frac{1}{NT}\sum_{t=1}^{T_i} \xi_{it}^d(\theta)^2$. The concentrated log-likelihood function is, therefore,

proportional to

$$\mathcal{L}(\theta) \propto \sum_{i=1}^{N}\sum_{t=1}^{T}\left\{\frac{s_{it}^d}{\sigma_\varepsilon}\Big(v_t(M_{it}^d s_{it}^d, d_{it}^d|\theta) - EV_t(M_{it}^d, s_{it}^d|\theta)\Big) - \frac{1}{2}\log\left(\sum_{i=1}^{N}\sum_{t=1}^{T}\xi_{it}^d(\theta)^2\right)\right\}, \tag{25}$$

where $EV_t(M_{it}^d, s_{it}^d|\theta)$ is the the logsum given in (14) evaluated at parameter value θ.[12] The parameter vector $\hat{\theta}$ that maximizes (25) is the ML estimator of the model parameters.

4.3 Taste Shocks as Unobserved State Variables

We are now ready to investigate the effects of smoothing on the accuracy of the ML estimator based on the DC-EGM algorithm. We conduct two Monte Carlo experiments where we vary the degree of smoothing induced by extreme value taste shocks and income uncertainty respectively. Throughout, we focus on estimating the parameter that index disutility of work, δ, while keeping all other fixed at their true values. The Appendix C contains average estimation time for the DC-EGM.

Taste Shocks and Approximation Error. Figure 7 displays the root mean square error (RMSE) of the parameter estimates for the disutility of work, $\hat{\delta}$. Results are shown for varying degree of smoothing, $\sigma_\varepsilon \in \{0.01, 0.05\}$, and different values of the disutility of work parameter, $\delta \in \{0.1, 0.5\}$. With RMSE around $1.0e^{-3}$, the proposed estimator is already accurate with 50 grid points and rapidly improves as the number of grid points increase from 50 through 1000. Note that standard errors will of course increase with σ_ε due to the increased amount of unexplained variation in the error term and RMSE reflects this too. Bearing this is mind, it is evident that the approximation bias decreases as the degree of smoothing increases, i.e., larger values of σ_ε. For higher levels of smoothing, problems with multiplicity of the Euler equation solutions disappear and few grid points are needed to approximate the (smooth) consumption function. This is particularly true when the disutility from work is large ($\delta = .5$) because the non-concave regions are larger in this case. We also calculated the Monte Carlo Standard Deviation (MCSD)[13], which is on the order $1.0e^{-4}$ irrespectively of the number of grid points used.

[12] Following (25), the logsum only has to be evaluated for workers, $s_{it}^d = 1$.
[13] MCSD results not shown

Figure 7: Monte Carlo results: disutility of work.

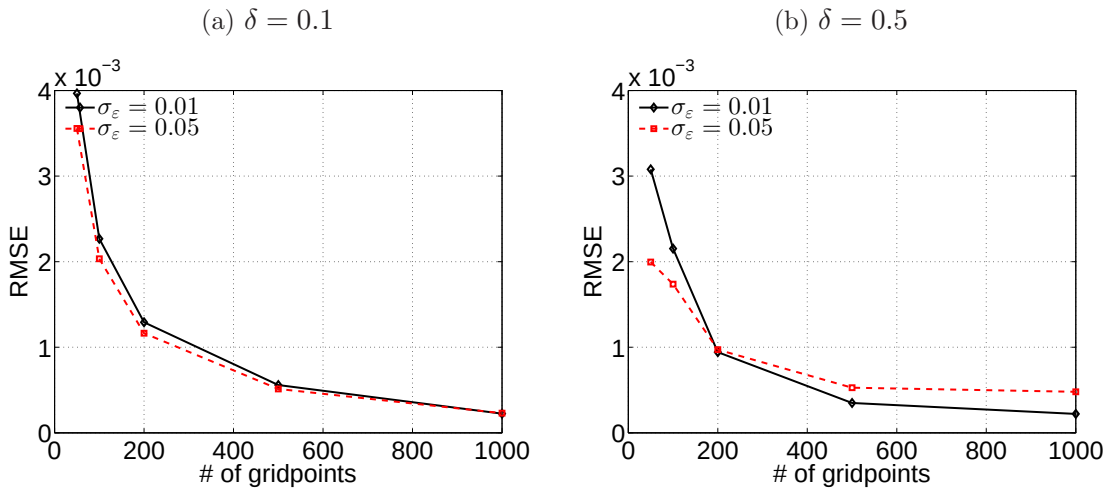

Notes: The plots illustrate the root mean square error (RMSE) of $\hat{\delta}$. Results are shown for varying degree of smoothing, $\sigma_\varepsilon \in \{0.01, 0.05\}$, and different values of the disutility of work, $\delta \in \{0.1, 0.5\}$. The rest of the parameters are at their baseline levels, see Table 1.

Income Uncertainty. Additional uncertainty about, e.g., future labor market income tend to smooth out *secondary* kinks stemming from multiple solutions to the Euler equations. To illustrate how that additional smoothing affects the proposed estimator, Figure 8 display RMSE when introducing *income uncertainty*. We report results from two different values of the income variance[14], $\sigma_\eta^2 \in \{0.001, 0.05\}$. The first level, 0.001, does not completely smooth out secondary kinks while the significantly more uncertain income process with $\sigma_\eta^2 = 0.05$ does (see the right panel of Figure 4).

Income uncertainty together with taste shocks smooth the problem to such a degree that the RMSE drops by an order of magnitude when increasing the income variance from .001 to 0.05. Hence, using only few grid points when estimating such a model will result in only minor approximation errors.

As mentioned, standard errors will of course increase with σ_ε due to the increased amount of unexplained variation. The MCSD is quite small and unaffected by the degree of income uncertainty as well as the number of grid points, but increases from 0.00023 to 0.00045 as σ_ε increases from 0.01 to 0.05. This is the main explanation for why RMSE is only smaller for a small

[14]The values of the income variance we use correspond well to the empirical findings, for example in Gourinchas and Parker (2002); Meghir and Pistaferri (2004); Imai and Keane (2004).

Figure 8: Monte Carlo results: income uncertainty.

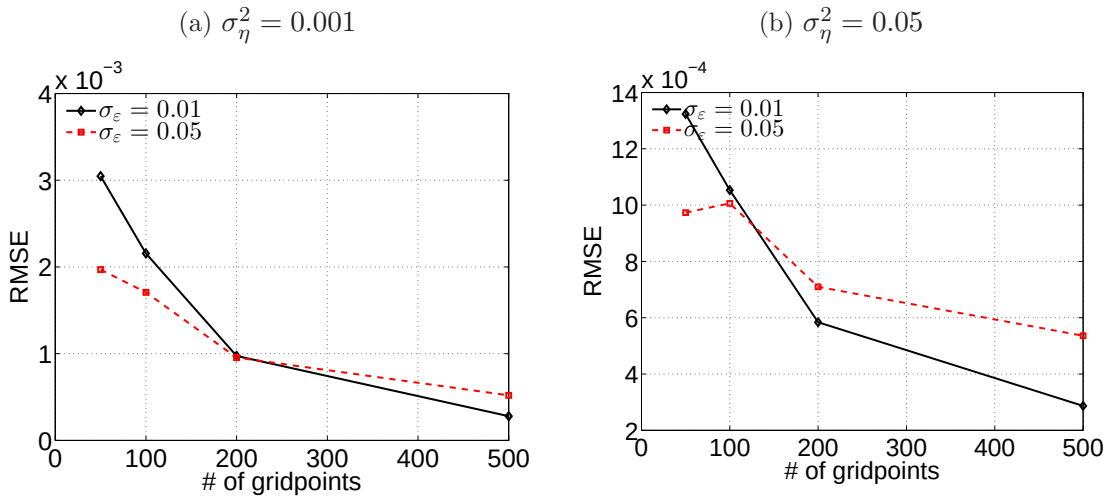

Notes: The plots illustrate the root mean square error (RMSE). Results are shown for varying degree of smoothing, $\sigma_\varepsilon \in \{0.01, 0.05\}$, and different values of the income variance, $\sigma_\eta^2 \in \{0.001, 0.05\}$. The rest of parameters are at their baseline levels, see Table 1.

number of grid points. Sorting out this effect its clear that increasing σ_ε decreases the amount of pure approximation bias - especially when the number of grid points is small. Note that MCSD is very small, in part due to a relatively large sample size, but also because the variance of the iid extreme value error term is extremely small. In most empirical applications, σ_ε would be larger; leading to an even smoother problem than the one we consider here. Hence, with relatively few grid points we can expect to obtain an even smaller approximation bias induced by the finite grid approximation in the DC-EGM.

4.4 Taste Shocks as Logit Smoother

Until now we have assumed that the correct model has unobserved state variables, and thus $\sigma_\varepsilon > 0$ has to be estimated. To investigate how the proposed estimator performs if the data stems from a model in which there are *no* unobserved states, we estimate versions of the model where we *impose* $\sigma_\varepsilon > 0$ and, thus, estimate a misspecified model. This is interesting because if researchers have reasons to believe that the underlying model has no shocks, the inclusion of these shocks acts as a smooth approximation to the true deterministic model. As argued above, solving the smoothed model is much faster since it requires fewer grid points and, thus, is much faster to estimate.

Figure 9 illustrates the RMSE when using 50, 100 and 500 grid points for various levels of

smoothing $\sigma_\varepsilon \in [0.001, 0.05]$ while the correct level is $\sigma_\varepsilon = 0$. Intuitively, as the model becomes "more" misspecified (increasing the imposed σ_ε), the RMSE and the MCSD increases. Interestingly, for a given number of discrete grid points, the RMSE is minimized by a $\sigma_\varepsilon > 0$. While large degree of smoothing induces significant approximation bias, the bias is initially falling in σ_ε until some point at which the RMSE increases again. The minimum of the RMSE is attained for lower levels of smoothing if additional stochasticity (i.e. income shocks) is present in the model. This is expected because the income uncertainty smooths the problem and less logit smoothing is needed to obtain the optimal smooth approximation. It is worth noting, however, that the optimal amount of logit smoothing may not be sufficient to completely eliminate the non-convexities in the model. It is therefore essential for the solution method to be able to robustly solve optimization problems with multiple local solutions, the task that DC-EGM performs particularly well.

These results show the potential for great speed gains by smoothing. Using only 50 grid points and imposing $\sigma_\varepsilon = 0.01$ produce a RMSE of around the same level as using 500 grid points and imposing $\sigma_\varepsilon \approx 0$ close to the true model. We can reduce the number of gridpoints by an order of magnitude without increasing the root mean square error significantly simply by choosing the degree of smoothing appropriately. Note, however, that there is naturally a trade-off between lowering the computational cost by increasing smoothing and decreasing the number of grid points and the accuracy of the resulting solution compared to the true solution of the non-smooth model.

5 Discussion and Conclusions

In this paper we have shown how complications from numerous discontinuities in the consumption function to a life cycle model with discrete and continuous choices can be avoided by smoothing the problem and using the DC-EGM algorithm. The proposed algorithm retains all the nice features of the original EGM method, namely that it typically does not require any iterative root-finding operations, and is equally efficient in dealing with borrowing constraints. Moreover, we show that the smoothed model can be successfully estimated by the NFXP estimator based on the DC-EGM algorithm even with small number of grid points, and even when the true DGP is non-smooth.

For expositional clarity, we focused on a simple illustrative example when explaining the details of the DC-EGM algorithm. This also allows us to derive an analytical solution that we can compare to the numerical one. The analytical solution provides economic intuition for why first

Figure 9: Monte Carlo results: true model without taste shocks (misspecified)

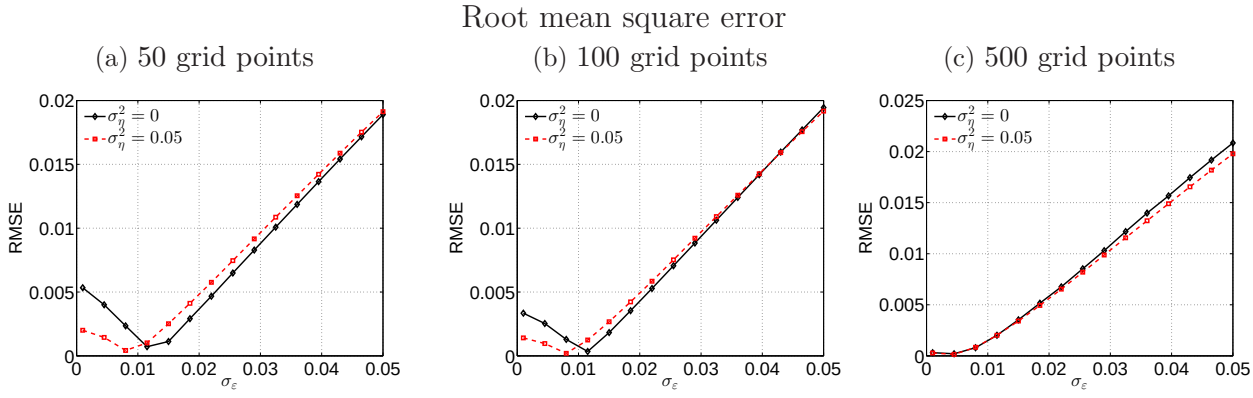

Notes: The plots illustrate the root mean square error (RMSE) from estimation of a *misspecified* model. The model from which data are simulated is deterministic, $\sigma_\varepsilon = 0$, while the model used to estimate the disutility of work imposes $\sigma_\varepsilon > 0$. Results are shown for varying degree of *imposed* smoothing, $\sigma_\varepsilon \in [0.001, 0.05]$ on the horizontal axes, different levels of income shocks, $\sigma_\eta \in \{0, 0.05\}$, and different number of grid points. The rest of parameters are at their baseline levels, see Table 1.

and second order kinks appear and permits direct evaluation of the precision of the DC-EGM algorithm. Admittedly, the illustrative model of consumption and retirement is very stylized, and the reader may wonder if DC-EGM can be used to solve and estimate larger, more complex and realistic models with more state variables, multiple discrete alternatives, heterogeneous agents, institutional constraints, etc.. The answer is positive. As shown in the Appendix A, the DC-EGM method can be applied to a much more general class of problems as long as the post decision state variable is a sufficient static for the continuous choice in the current period, and the marginal utility function and intra-temporal budget constraint are invertible. When the marginal utility function is *analytically* invertible, DC-EGM also avoids the bulk of costly root-finding operations.[15]

The DC-EGM method has been implemented in several recent empirical applications, where it has proven to be a powerful tool for solving and estimating more complex DC models in various fields: labor supply, human capital accumulation and saving (Iskhakov and Keane, 2016); joint retirement decision of couples (Jørgensen, 2014); consumption, housing purchases and housing debt (Yao, Fagereng and Natvik, 2015); saving decisions and fertility (Ejrnæs and Jørgensen, 2015); precautionary borrowing and credit card debt (Druedahl and Jørgensen, 2015).

[15]DC-EGM algorithm can also be generalized for other specifications including the models with large state space and multidimensional discrete choice. White (2015); Iskhakov (2015); Druedahl and Jørgensen (2016) present theoretical foundations for extending endogenous grid methods to multi-dimensional models.

We have demonstrated in the Monte Carlo experiments that the NFXP maximum likelihood estimator based on the DC-EGM solution algorithm performs very well when decisions are made under uncertainty, e.g. in the presence of extreme valued taste shocks and the existence of income uncertainty. Even when the true model is deterministic, taste shocks can be used as a powerful smoothing device to simplify the solution without much approximation bias due to over-smoothing.

The addition of extreme value taste shocks is not only a convenient smoothing device that simplifies the solution of DC models, it is also an empirically relevant extension required to avoid statistical degeneracy of the model. In empirical applications the variance of these shocks is typically much larger compared to what we have considered here. This makes models smooth enough to almost eliminate approximation bias in parameter estimates even with relatively few grid points. We therefore conclude that DC-EGM is both practical and appears to be a fast and accurate method for use in actual empirical applications.

However from the standpoint of using DC-EGM to find highly accurate solutions to DC problems, while the results we present in this paper are highly encouraging, our conclusions are based on comparing the numerical solution to an analytical solution of a *particular* DC problem. It would be much better to be able to *prove* that DC-EGM provides similar accuracy for an entire *class* of DC problems. Ideally this would be done by deriving bounds on the error between the true decision rule and the approximate decision rule computed by DC-EGM. We conjecture that these bounds, dependent on the number of endogenous gridpoints n used in the DC-EGM algorithm, would converge to zero as $n \to \infty$. We are not aware of any error bounds or convergence proofs even in more straightforward case of concave dynamic problems with only continuous choice that EGM was originally developed for by Carroll (2006). We believe the uniform bounds we derived for the approximation error involved in the use of extreme value smoothing of DC problems may provide one of the tools to derive bounds on the error between the true decision rules and the approximate decision rules calculated by DC-EGM.

A Theoretical foundations of DC-EGM

For the purpose of this Appendix we consider the following more general formulation of the consumption/savings and retirement problem. Let M_t denote consumable wealth that is continuous state variable with particular motion rule described below, and let s_t denote a vector of additional discrete or discretized state variables. Let c_t be the scalar continuous decision (consumption) and d_t be a scalar discrete decision variable with finite set of values that could encode multiple dis-

crete decisions if needed. Consider the dynamic discrete-continuous choice problem given by the Bellman equation,

$$V_t(M_t, s_t) = \max_{0 \leq c_t \leq M_t, d_t \in D_t} \Big[u(c_t, d_t, s_t) + \sigma_\varepsilon \varepsilon_t(d_t) + \beta_t E_t \big\{ V_{t+1}(M_{t+1}, s_{t+1}) | A_t, d_t \big\} \Big], \tag{26}$$

where $t = 1, \ldots, T-1$, and the last component of the maximand is absent for $t = T$. The choices in the model are restricted by the credit constraint $c_t < M_t$ and feasibility sets D_t. The per period utility includes scaled taste shocks $\sigma_\varepsilon \varepsilon_t(d_t)$, where ε_t is a vector of i.i.d. Extreme Value (Type I) distributed random variables. The dimension of ε_t is equal to the number of alternatives that the discrete choice variable may take, $\varepsilon_t(d_t)$ denotes the component that corresponds to a particular discrete decision. In the general case the discount factor β_t is time-specific to allow for the probability of survival. The expectation is taken over the taste shocks ε_{t+1}, transition probabilities of the state process s_t as well as any serially uncorrelated (or idiosyncratic) shocks that may affect M_{t+1} and s_{t+1}. The expectation is taken conditional on the choices in period t using the *sufficient statistic* $A_t = M_t - c_t$ in place of the continuous (consumption) choice.

Using the well known representation of the expectation of the maximum of Extreme Value distributed random variables, the Bellman equation (26) can be written in terms of the deterministic choice-specific value functions $v_t(M_t, s_t | d_t)$ as

$$\begin{aligned} v_t(M_t, s_t | d_t) &= \max_{0 \leq c_t \leq M_t} \Big[u(c_t, d_t, s_t) + \beta_t E_t \big\{ V_{t+1}(M_{t+1}, s_{t+1}) | A_t, d_t \big\} \Big] & (27) \\ &= \max_{0 \leq c_t \leq M_t} \Big[u(c_t, d_t, s_t) + \beta_t E_t \Big\{ \phi\big(v_{t+1}(M_{t+1}, s_{t+1} | d_{t+1}), D_{t+1}, \sigma_\varepsilon\big) | A_t, d_t \Big\} \Big], & (28) \end{aligned}$$

where $\phi(x_j, J, \sigma) = \sigma \log \left[\sum_{j \in J} \exp \frac{x_j}{\sigma} \right]$ is the logsum function. The expectation in (28) is now only taken w.r.t. state transitions and idiosyncratic shocks, unlike in (26) and (27).

The crucial assumption for the DC-EGM is that *post decision* state A_t constitutes the sufficient statistic for the continuous choice in period t, i.e. that transition probabilities/densities of the state process (M_t, s_t) depend on A_t rather than M_t or c_t directly. It is also required that A_t as a function of M_t is (analytically) invertible. For our case, assume for concreteness that $A_t = M_t - c_t$, and that $M_{t+1} = RA_t + y(d_t)$, where R is a gross return, and $y(d_t)$ is discrete choice specific income. We also assume that the utility function $u(c_t, d_t, s_t)$ satisfies the following condition.

Assumption 1 (Concave utility)**.** The instantaneous utility $u(c_t, d_t, s_t)$ is concave[16] in c_t and has a monotonic derivative w.r.t. c_t that is (analytically) invertible.

Lemma 1 (Smoothed Euler equation)**.** *The Euler equation for the problem* (26) *takes the form*

$$u'(c_t, d_t, s_t) = \beta_t R \mathbb{E}_t \left[\sum_{d_{t+1} \in D_{t+1}} u'\big(c_{t+1}(M_{t+1}, s_{t+1} | d_{t+1}), d_{t+1}, s_{t+1}\big) P_{t+1}\big(d_{t+1} | M_{t+1}, s_{t+1}\big) \right] \tag{29}$$

where $u'(c_t, d_t, s_t)$ is the partial derivative of the utility function w.r.t. c_t, $c_{t+1}(M_{t+1}, s_{t+1} | d_{t+1})$ is the choice-specific consumption function in period $t+1$, and $P_{t+1}(d_{t+1} | M_{t+1}, s_{t+1})$ is the conditional

[16] More precisely, a weaker condition is sufficient, namely for every x and arbitrary $\Delta_1 > 0$ and $\Delta_2 > 0$ it must hold that $u(c_t + \Delta_1, d_t, s_t) - u(c_t, d_t, s_t) \geq u(c_t + \Delta_1 + \Delta_2, d_t, s_t) - u(c_t + \Delta_2, d_t, s_t)$, see Theorem 2.

discrete choice probability in period $t+1$, given by

$$P_t(d_t|M_t, s_t) = \exp\big(v_t(M_t, s_t|d_t)/\sigma_\varepsilon\big) \Big/ \sum_{d\in D_t} \exp\big(v_t(M_t, s_t|d)/\sigma_\varepsilon\big). \tag{30}$$

Proof. Discrete choice specific consumption functions $c_t(M_t, s_t|d_t)$ satisfy the the first order conditions for the maximization problems in (27) given by

$$u'(c_t, d_t, s_t) + \beta_t E\left\{\frac{\partial V_{t+1}(M_{t+1}, s_{t+1})}{\partial M_{t+1}}\frac{\partial M_{t+1}}{\partial c_t}\right\} = 0 \tag{31}$$

for every value of $d_t \in D_t$. The envelope conditions for (27)

$$\frac{\partial v_t(M_t, s_t|d_t)}{\partial M_t} = \beta_t E\left\{\frac{\partial V_{t+1}(M_{t+1}, s_{t+1})}{\partial M_{t+1}}\frac{\partial M_{t+1}}{\partial M_t}\right\}, \tag{32}$$

and because $\partial M_{t+1}(d_t)\big/\partial M_t = R = -\partial M_{t+1}(d_t)\big/\partial c_t$, it holds for all d_t and $t = 1, \ldots, T-1$

$$u'(c_t, d_t, s_t) = \frac{\partial v_t(M_t, s_t|d_t)}{\partial M_t}. \tag{33}$$

The first order condition for (28) is

$$u'(c_t, d_t, s_t) = \beta_t R\mathbb{E}_t\left[\sum_{d_{t+1}\in D_{t+1}} \frac{\partial v_{t+1}(M_{t+1}, s_{t+1}|d_{t+1})}{\partial M_{t+1}} P_{t+1}\big(d_{t+1}|M_{t+1}, s_{t+1}\big)\right], \tag{34}$$

where choice probabilities $P_{t+1}\big(d_{t+1}|M_{t+1}, s_{t+1}\big)$ are given by (30). Plugging (33) into (34) completes the proof. □

The DC-EGM algorithm outlined in Algorithm 3 is readily applicable to the general formulation of the discrete-continuous problem (26), expect for the extra loop that has to be taken over all additional states s_t in Step 3 (Algorithm 3). The expectation over the transition probabilities of the state process is calculated together with the expectation over the other stochastic elements of the model in Algorithm 1.

The criteria for selecting the solutions of the Euler equation that correspond to the optimal behavior in the model is based on the monotonicity of the savings function, which is established with the following theorem[17].

Theorem 2 (Monotonicity of savings function) *Denote $A_t(M_t, s_t|d_t) = M_t - c_t(M_t, s_t|d_t)$ a discrete choice specific savings function in period t. Under the Assumption 1, function $A_t(M, s_t|d_t)$ is monotone non-decreasing in M for all t,s_t and $d_t \in D_t$.*

Proof. Theorem 2 is an application of Theorem 4 in Milgrom and Shannon (1994) to the current problem. Conditional savings function $A_t(M_t, s_t|d_t)$ is a maximizer in the expression similar to (27) for the discrete choice specific value function $v_t(M_t, s_t|d_t)$. As a function of M and A, the maximand in this expression is given by

$$f(A, M) = u(M - A, d_t, s_t) + \beta_t E_t\big\{V_{t+1}(M_{t+1}(A), s_{t+1})\big\} \tag{35}$$

[17] A similar monotonicity result is also used in Fella (2014).

where $M_{t+1}(A)$ is next period wealth as an *increasing* function of A. It is necessary and sufficient to show that $f(A, M)$ is quasisupermodular in A and satisfies the single crossing property in (A, M). The former is trivial because A is a scalar. For the latter consider $A' > A''$, $M' > M''$ and assume $f(A', M'') > f(A'', M'')$. Then

$$\begin{gathered} f(A', M') - f(A'', M') = \\ = u\left(M' - A', d_t, s_t\right) - u\left(M' - A'', d_t, s_t\right) + \\ +\beta_t \left[EV_{t+1}\left(M_{t+1}(A'), s_{t+1}\right) - EV_{t+1}\left(M_{t+1}(A''), s_{t+1}\right)\right] \geq \\ \geq u\left(M'' - A', d_t, s_t\right) - u\left(M'' - A'', d_t, s_t\right) + \\ +\beta_t \left(EV_{t+1}\left(M_{t+1}(A'), s_{t+1}\right) - EV_{t+1}\left(M_{t+1}(A''), s_{t+1}\right)\right) = \\ f(A', M'') - f(A'', M'') > 0. \end{gathered} \tag{36}$$

For the first inequality we use

$$\begin{gathered} u\left(M' - A', d_t, s_t\right) - u\left(M' - A'', d_t, s_t\right) \geq u\left(M'' - A', d_t, s_t\right) - u\left(M'' - A'', d_t, s_t\right), \\ u\left(M' - A', d_t, s_t\right) - u\left(M'' - A', d_t, s_t\right) \geq u\left(M' - A'', d_t, s_t\right) - u\left(M'' - A'', d_t, s_t\right), \\ u\left(z, d_t, s_t\right) - u\left(z - \Delta_M, d_t, s_t\right) \geq u\left(z + \Delta_A, d_t, s_t\right) - u\left(z + \Delta_A - \Delta_M, d_t, s_t\right), \end{gathered} \tag{37}$$

where $z = M' - A'$, $\Delta_A = A' - A'' > 0$, $\Delta_M = M' - M'' > 0$, and which is due to Assumption 1, i.e. concavity of the utility function. It follows then that $f(A', M') > f(A'', M')$. Similarly, assumption $f(A', M'') \geq f(A'', M'')$ leads to $f(A', M') \geq f(A'', M')$, and thus $f(A, M)$ satisfies the single crossing property, and monotonicity theorem in Milgrom and Shannon (1994) applies. □

B Spurious Discontinuities from Numerical Integration

To illustrate how naive numerical quadrature integration can produce spurious discontinuities in the policy function, we here focus on the illustrative model without smoothing. Particularly, for working households, the smoothed Euler equation in (16) collapses to

$$\begin{aligned} u'\left(c_t\left(M_t|d_t\right)\right) &= \beta \int_0^\infty Ru'(c_{t+1}(M_{t+1}|d_{t+1}=1)) \cdot \mathbf{1}\{M_{t+1} \leq \overline{M}_{t+1}\} f(d\eta) \\ &+ \beta \int_0^\infty Ru'(c_{t+1}(M_{t+1}|d_{t+1}=0)) \cdot \mathbf{1}\{M_{t+1} > \overline{M}_{t+1}\} f(d\eta). \end{aligned} \tag{38}$$

where we recall that $M_{t+1} = R\left(M_t - c_t\left(M_t|d_t\right)\right) + y\eta$. With the change of variables, $q = f(\eta)$, we can write the Euler equation (38) as

$$\begin{aligned} u'\left(c_t\left(M_t|d_t\right)\right) &= \beta \int_0^{\overline{q}_t} f^{-1}(q) u'\left(c_{t+1}\left(R(M_t - c_t(M_t|d_t)) + y f^{-1}(q), d_{t+1}=1\right)\right) dq \\ &+ \beta \int_{\overline{q}_t}^1 f^{-1}(q) u'\left(c_{t+1}\left(R(M_t - c_t(M_t|d_t)) + y f^{-1}(q), d_{t+1}=0\right)\right) dq \end{aligned} \tag{39}$$

where the threshold $\overline{q}_t$ is given by

$$\overline{q}_t = f\left(\frac{\overline{M}_{t+1}}{M_{t+1}}\right). \tag{40}$$

As long as the income shock distribution is not degenerate, the resulting Euler equation (39) is continuous and smooth in $c_t(M_t, \mathbb{W})$ through M_{t+1} in spite of the discontinuity in the consumption function $c_{t+1}(M_{t+1}, \mathbb{W})$ at $M_{t+1} = \overline{M}_{t+1}$. In turn, this suggests that numerical integration should be done twice – once for each case – to ensure that the integral is well-behaved.

In contrast, the naive Euler equation in (38) is discontinuous in $c_t(M_t, \mathbb{W})$. When using numerical quadrature to evaluate the integral, for a given level of resources, some of the nodes will result in $M_{t+1} \leq \overline{M}_{t+1}$ while others will result in the opposite case. For concreteness, say that 10 nodes are used and the five lowest nodes results in $M_{t+1} \leq \overline{M}_{t+1}$. Say also that for a slightly larger value of current resources perhaps only four nodes satisfy $M_{t+1} \leq \overline{M}_{t+1}$ while now six invokes the alternative. When comparing the solution found in the two (close) values of current period resources, there will be a discontinuous change in the optimal consumption. In the current model, this would result in spurious downward kinks in the consumption function around a secondary kink, as illustrated in the left panel of Figure 3.

C DC-EGM run times

Figure 10 illustrates the average estimation time spent to estimate $\hat{\delta}$. Results are shown for varying degree of income uncertainty, $\sigma_\eta \in \{0.001, 0.05\}$, and different values of the disutility of work parameter, $\delta \in \{0.1, 0.5\}$

Figure 10: Timing: income uncertainty.

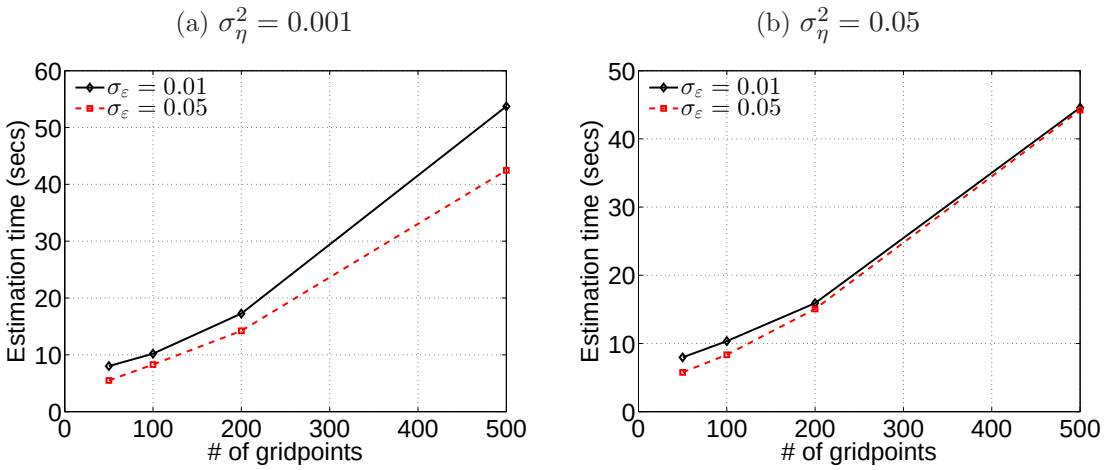

Notes: The plots illustrate the time spent to estimate the model. Results are shown for varying degree of smoothing, $\sigma_\varepsilon \in \{0.01, 0.05\}$, and different values of the income variance, $\sigma_\eta^2 \in \{0.001, 0.05\}$. The rest of parameters are at their baseline levels, see Table 1.

D Proof of Extreme Value Homotopy Principle

This appendix proves Theorem 3 which states that the value function and optimal decision rules in the presence of Type I extreme value distributed taste shocks converge (in an appropriate sense to be defined below) to the value functions and decision rules of a limiting problem without

taste shocks. We prove Theorem 3 for a more general class of problems than just the retirement consumption model, and therefore restate it below.

Let ε be a random variable having a standardized Type I extreme value distribution with CDF $F(\varepsilon)$ given by

$$F(\varepsilon) = \exp\{-\exp\{-\varepsilon\}\}. \tag{41}$$

We have $E\{\varepsilon\} = \gamma$, where $\gamma = 0.577\ldots$ is Euler's constant and $\text{var}(\varepsilon) = \pi^2/6$. Then if σ is a positive scaling constant, $\sigma\varepsilon$ will also be a Type I extreme value distribution with expected value $\sigma\gamma$ and variance $\sigma^2\pi^2/6$. In the notation of the illustrative model in the paper, σ corresponds to the scaling parameter of the "perturbed" model σ_ε.

The homotopy convergence result we prove below holds for a considerably more general class of dynamic programming problems than the simple retirement example we analyzed in section 2.1 or even the class defined in Appendix A, where we assumed the continuous choice is a unidimensional variable and we imposed additional assumptions to ensure monotonicity of the savings function. In this appendix we consider a more general class of problems, though we do not strive for maximum possible generality in order to make our proof as straightforward as possible.

Consider a finite horizon DP problem without Type I extreme value taste shocks which we also refer to as the "unperturbed" DP problem. In the last period, T, the agent chooses a vector of k continuous choice variables $c \in C_T(d,s)$, where $C_T(d,s)$ is a compact subset of a R^k and d is one of the discrete choices and s is a potentially multidimensional vector of state variables in some Borel subset S of a finite dimensional Euclidean space. We assume that the discrete choice d is an element of a finite choice set $D_T(s)$. Let $u_T(d,c,s)$ be a utility function that is continuous in c for each s and each $d \in D_T(s)$ and a Borel measurable function of s for each c and d. Then the value function in period T is $V_T(s)$ given by

$$V_T(s) = \max_{d\in D_T(s)} \max_{c\in C_T(d,s)} u_T(d,c,s). \tag{42}$$

Now consider time $T-1$ and let $p_T(s'|s,c,d)$ be a Markov transition probability providing the conditional probability distribution over the state s' at time T given that the state vector at time $T-1$ is s, the discrete choice is d, and the continuous choice is c. Define the conditional expectation of V_T, $EV_{T-1}(d,c,s)$, by

$$EV_{T-1}(d,c,s) = \int V_T(s')p_T(\partial s'|d,c,s) \tag{43}$$

where we use $\partial s'$ to indicate the stochastic next period state variables over which this expectation is taken. In Assumption C below, we assume that this conditional expectation exists and is continuous in c for each $s \in S$ and $d \in D_{T-1}(s)$. Then by backward induction we can define the value function $V_{T-1}(s)$ and, continuing for each $t \in \{T-1, T-2, \ldots, 0\}$ we can define the sequence of functions $\{V_t\}$ recursively using Bellman's equation

$$V_t(s) = \max_{d\in D_t(s)} \max_{c\in C_t(d,s)} \left[u_t(d,c,s) + \beta \int V_{t+1}(s')p_{t+1}(\partial s'|d,c,s)\right]. \tag{44}$$

where $\beta \geq 0$ is the agent's discount factor.

We make the following assumptions on this limiting DP problem without taste shocks that is sufficient to guarantee the existence of a well defined solution.

Assumption B *The choice sets $D_t(s)$ are all finite with a uniformly bounded number of elements*

D given by

$$D = \max_{t\in\{0,1,\ldots,T\}} \sup_{s\in S} |D_t(s)| < \infty \tag{45}$$

where $|D_t(s)|$ denotes the number of elements in the finite set $D_t(s)$.

Assumption C *For each $t \in \{0, 1, \ldots, T\}$ and each $s \in S$ and each $d \in D_t(s)$ the function $u_t(d, c, s)$ is continuous in c, and for each $t \in \{1, 2, \ldots, T-1\}$, $s \in S$ and $d \in D_{t-1}(s)$ the function $EV_t(d, c, s)$ is given by*

$$EV_t(d, c, s) = \int V_t(s')p_t(\partial s'|d, c, s) \tag{46}$$

is finite and continuous in c.

Define the *discrete choice-specific continuous choice function* $c_t(d, s)$ by

$$c_t(d, s) = \underset{c\in C_t(d,s)}{argmax} \left[u_t(d, c, s) + \beta EV_{t+1}(d, c, s)\right] \tag{47}$$

and the optimal discrete decision rule $\delta_t(s)$ by

$$\delta_t(s) = \underset{d\in D_t(s)}{argmax} \left[u_t(d, c_t(d, s), s) + \beta EV_{t+1}(d, c_t(d, s), s)\right]. \tag{48}$$

The overall optimal continuous decision rule $c_t(s)$ is then given by

$$c_t(s) = c_t(\delta_t(s), s). \tag{49}$$

The *solution* to the DP problem is given by the collection Γ of the $T + 1$ value functions $\{V_0, V_1, \ldots, V_T\}$, the $T + 1$ optimal continuous decision rules $\{c_0, c_1, \ldots, c_T\}$ and the $T + 1$ optimal discrete decision rules $\{\delta_0, \delta_1, \ldots, \delta_T\}$.

Now we define a family of *perturbed* DP problems index by σ, the scale parameter of the Type I Extreme value distribution. Let ε denote a *vector* of *IID* extreme value random variables with the same dimension as $|D_t(s)|$, the number of elements in the finite choice set $D_t(s)$. Assume the elements of $D_T(s)$ are ordered in some fashion and let $\varepsilon(d)$ be the component of the vector ε corresponding to the choice of alternative $d \in D_t(s)$. We will refer to $\varepsilon(d)$ as the "d^{th} taste shock".

Now consider the last period T. The value function $V_{\sigma,T}(s, \varepsilon)$ is given by

$$V_{\sigma,T}(s, \varepsilon) = \max_{d\in D_T(s)} \max_{c\in C_T(d,s)} \left[u_T(d, c, s) + \sigma\varepsilon(d)\right]. \tag{50}$$

Notice that $V_{\sigma,T}$ is now a function of the vector s and the vector $\varepsilon \in R^{|D_T(s)|}$. If the number of elements of $D_T(s)$ varies with $s \in S$ we can embed the vector ε in R^D where D is the upper bound on the number of discrete choices by Assumption. We can use the convention that if $|D_T(s)| < D$ for some $s \in S$, the function $V_{\sigma,T}(s, \varepsilon)$ depends only on the components of ε corresponding to the feasible choices $d \in D_T(s)$ and not on any components d that are not elements of $D_T(s)$.

The CDF $F(\varepsilon)$ of the vector random variable ε is given by the product of the univariate Type I Extreme value CDFs, i.e.

$$F(\varepsilon_1, \ldots, \varepsilon_D) = \prod_{d=1}^{D} \exp\{-\exp\{-\varepsilon(d)\}\} \tag{51}$$

To compute the expected value of $V_T(s,\varepsilon)$ we apply multivariate integration to get

$$\begin{aligned} EV_{\sigma,T}(d,c,s) &= \int_{s'}\int_{\varepsilon'} V_t(s',\varepsilon')F(\partial\varepsilon')p_T(\partial s'|d,c,s) \\ &= \int_{s'} \sigma \log\left(\sum_{d\in D_T(s')} \exp\{u_T(d,c_T(s,d),d)/\sigma\}\right) p_T(\partial s'|d,c,s) \end{aligned} \tag{52}$$

where $c_T(s,d) = argmax_{c\in C_T(d,s)}\, u_T(d,c,s)$ is the choice-specific continuous choice function. The closed form expression for the expectation over ε' the Type I extreme value random variables is a consequence of a property of extreme value random variables known as *max-stability* i.e. the maximum of a finite collection of Type I extreme value random variables has a (shifted) Type I extreme value distribution. We refer to the log-sum formula inside the integral of the lower equation of (52) as the *smoothed max function.* We now prove a key Lemma that establishes a bound between the usual max function and the smoothed max function.

Lemma 2 (Logsum error bounds)**.** *Let $\{v_1,\ldots,v_D\}$ be any finite set of D real numbers and let $\sigma > 0$ be a constant. Then we have*

$$0 \leq \sigma \log\left(\sum_{d=1}^{D} \exp\{v_d/\sigma\}\right) - \max\{v_1,\ldots,v_D\} \leq \sigma\log(D). \tag{53}$$

Proof. Consider the shifted values $v_d - \max(v_1,\ldots,v_D) \leq 0$. It follows that

$$\log\left(\sum_{d=1}^{D} \exp\{(v_d - \max\{v_1,\ldots,v_D\})/\sigma\}\right) \leq \log\left(\sum_{d=1}^{D}\exp\{0\}\right) = \log(D). \tag{54}$$

Define $d^* = \arg\max_d(v_d)$ and let $J \geq 1$ denote the number of elements of D for which $v_d = v_{d^*}$. The lower bound is obtained from observing that

$$\log\left(J + \sum_{d=1,d\neq d^*}^{D} \exp\{(v_d - \max\{v_1,\ldots,v_D\})/\sigma\}\right) \geq 0. \tag{55}$$

Combining (54) and (55) with the identity

$$\sigma\log\left(\sum_{d=1}^{D} \exp\{(v_d - \max\{v_1,\ldots,v_D\})/\sigma\}\right) = \sigma\log\left(\sum_{d=1}^{D}\exp\{v_d/\sigma\}\right) - \max\{v_1,\ldots,v_D\} \tag{56}$$

concludes the proof. □

Lemma 2 is the key to all of our subsequent results and the key to Theorem 2 since it shows that the difference between the max function and the smoothed max function is bounded by $\sigma\log(D)$ and this tends to 0 as $\sigma \downarrow 0$. This will imply that the difference between the value functions and decision rules of the unperturbed limiting DP problem and the family of perturbed DP problems with extreme value distributed taste shocks will converge to zero as the scale of the extreme value taste shocks, σ converges to 0.

We can now define the value functions at all time periods for the perturbed problem as the sequence $\{V_{\sigma,0}, \ldots, V_{\sigma,T}\}$ where $V_{\sigma,T}$ is given by equation (50) and the other value functions are given by the Bellman recursion

$$V_{\sigma,t}(s,\varepsilon) = \max_{d \in D_t(s)} \max_{c \in C_t(d,s)} \left[u_t(d,c,s) + \sigma\varepsilon(d) + \beta EV_{t+1}(d,c,s) \right] \tag{57}$$

where $EV_{\sigma,t+1}(d,c,s)$ is the conditional expectation of $V_{\sigma,t+1}(s,\varepsilon)$ and is given by

$$EV_{\sigma,t+1}(d,c,s) = \sigma \int_{s'} \log \left(\sum_{d' \in D_{t+1}(s')} \exp\{v_{\sigma,t+1}(d', c_{\sigma,t+1}(d',s'), s')/\sigma\} \right) p_{t+1}(\partial s' | d,c,s), \tag{58}$$

where

$$v_{\sigma,t+1}(d,c,s) = u_{t+1}(d,c,s) + \beta EV_{\sigma,t+2}(d,c,s) \tag{59}$$

and $c_{\sigma,t+1}(d,s)$ is the choice-specific continuous choice rule given by

$$c_{\sigma,t+1}(d,s) = \underset{c \in C_{t+1}(d,s)}{argmax} \left[v_{\sigma,t+1}(d,c,s) \right]. \tag{60}$$

Note that we used the Williams-Daly-Zachary Theorem again to obtain the expression for $EV_{t+1}(d,c,s)$ in equation (58) and we also note that due to the assumption that taste shocks are not only contemporaneously independent across different discrete choices d but also *intertemporally independent* processes, it follows that the value of the ε state vector at time t does not affect the conditional expectation of $V_{\sigma,t+1}$, and hence does not enter the conditional expectation $EV_{t+1}(d,c,s)$. This *conditional independence restriction* on the ε shocks is critical to all results that follow below.

Having defined the set of value functions for the family of perturbed problems we can define the full solution of the perturbed problem as the collection Γ_σ consisting of the value functions $(V_{\sigma,0}, \ldots, V_{\sigma,T})$, the continuous decision rules $(c_{\sigma,0}, \ldots, c_{\sigma,T})$ and the the discrete decision rules $(\delta_{\sigma,0}, \ldots, \delta_{\sigma,T})$. Note that all of these objects depend on both s and ε, which constitute the full vector of state variables in the perturbed problem. In particular, the discrete decision rule $\delta_{\sigma,t}(s,\varepsilon)$ can be defined using the choice-specific continuous choice rule $c_{\sigma,t}(d,s)$ as

$$\delta_{\sigma,t}(s,\varepsilon) = \underset{d \in D_t(s)}{argmax} \left[v_{\sigma,t}(d, c_{\sigma,t}(d,s), s) + \sigma\varepsilon(d) \right], \tag{61}$$

and the unconditional or continuous decision rule can be defined using the choice-specific continuous choice rules by

$$c_{\sigma,t}(s,\varepsilon) = c_{\sigma,t}(\delta_{\sigma,t}(s,\varepsilon), s). \tag{62}$$

To define a notion of convergence of the solution Γ_σ of the family of perturbed DP problems to the solution Γ of the limiting un-perturbed problem, we have to confront the difficulty that the state space for the family of perturbed problems is the set of points of the form (s,ε) for $s \in S$ and $\varepsilon \in R^D$ whereas the state space of the limiting unperturbed problem is just S. We start by noting the following representation for the value functions of the perturbed problem

$$V_{\sigma,t}(s,\varepsilon) = \max_{d \in D_t(s)} \left[v_{\sigma,t}(d, c_{\sigma,t}(d,s), s) + \sigma\varepsilon(d) \right], \tag{63}$$

which follows directly from the Bellman equation (57) and the definition of the v_t function in equation (59). We now compute a *partial expectation* of the value functions $V_{\sigma,t}(s,\varepsilon)$ over the ε holding the s state variable fixed. That is we define the partial expectation $EV_{\sigma,t}(s)$ as the function given by

$$\begin{aligned} EV_{\sigma,t}(s) &= \int_{\varepsilon} V_{\sigma,t}(s,\varepsilon)F(\varepsilon) \\ &= \sigma\left(\sum_{d\in D_t(s)} \exp\{v_{\sigma,t}(d,c_{\sigma,t}(d,s),s)/\sigma\}\right). \end{aligned} \tag{64}$$

We are in the position now to state the main result which is a reformulation of Theorem 3 for a more general class of DC models than the consumption retirement model in Section 2.

Theorem 2 (Extreme Value Homotopy Principle)**.** *Under assumptions* **B** *and* **C** *above, let*

$$\Gamma = \{(V_0,\ldots,V_T),(\delta_0,\ldots,\delta_T),(c_0,\ldots,c_T)\} \tag{65}$$

be the solution to the limiting DP problem without taste shocks given in equations (42), (44), (47) and (48) above. Similarly, let

$$\Gamma_\sigma = \{(V_{\sigma,0},\ldots,V_{\sigma,T}),(\delta_{\sigma,0},\ldots,\delta_{\sigma,T}),(c_{\sigma,0},\ldots,c_{\sigma,T})\} \tag{66}$$

be the solution to the the perturbed DP problem with Type I extreme value taste shocks with scale parameter $\sigma > 0$ given in equations (50), (57), (58), (61) and (62). Then as $\sigma \to 0$ we have

$$\lim_{\sigma\downarrow 0}\Gamma_\sigma = \Gamma, \tag{67}$$

where the convergence of value functions is defined in terms of the partial expectations of the value functions for the perturbed problems with taste shocks, $EV_{\sigma,t}(s)$ given in equation (64) so that we have uniform bound

$$\forall t \quad \sup_{s\in S}|EV_{\sigma,t}(s) - V_t(s)| \leq \sigma\left[\sum_{j=0}^{T-t}\beta^j\right]\log(D), \tag{68}$$

and the decision rules converge pointwise for all (s,ε), $s\in S$ and $\varepsilon\in R^D$, i.e.

$$\begin{aligned} \lim_{\sigma\downarrow 0}\delta_{\sigma,t}(s,\varepsilon) &= \delta_t(s) \\ \lim_{\sigma\downarrow 0}c_{\sigma,t}(s,\varepsilon) &= c_t(s), \end{aligned} \tag{69}$$

assuming that the decision rules of the limiting problem $\delta_t(s), c_t(s)$ are singletons, otherwise the limits are elements of the sets $(\delta_t(s), c_t(s))$.

Proof. We prove Theorem 2 in three steps. First, we prove (68) by induction using Lemma 2 and showing that the bounds are independent of s. Second, we prove convergence of decision rules assuming that the limiting problem Γ has unique solution. Third, we extend the latter result to non-singleton solution sets.

Lemma 3 (DP error bounds)**.** *Let $V_t(s)$ be the value function for the unperturbed DP problem and let $EV_{\sigma,t}(s)$ be the partial expectation of the value function $V_{\sigma,t}(s,\varepsilon)$ to the perturbed DP problem.*

Then we have

$$\forall t, s \;\; 0 \leq EV_{\sigma,t}(s) - V_t(s) \leq \sigma \left[\sum_{j=0}^{T-t} \beta^j \right] \log(D). \tag{70}$$

Lemma 3 can be proved by induction using Lemma 2. We work out the first several steps of the inductive argument, starting at period T. In period T $V_T(s)$ is given by equation (42), which can be rewritten in terms of the choice-specific continuous choice rule as

$$V_T(s) = \max_{d \in D_T(s)} [u_T(d, c_T(d, s), s)] \tag{71}$$

and similarly, we have $EV_{\sigma,T}(s)$ is given by

$$EV_{\sigma,T}(s) = \sigma \log \left(\sum_{d \in D_T(s)} \exp\{u_T(d, c_T(d, s), s)/\sigma\} \right), \tag{72}$$

since it is easy to see that $c_T(d, s) = c_{\sigma,T}(d, s)$ in the final period T. Using Lemma 2, we obtain the bounds

$$0 \leq EV_{\sigma,T}(s) - V_T(s) \leq \sigma \log(D), \; \forall s \in S, \tag{73}$$

which establishes the base case for our induction proof. Now suppose the inductive hypothesis holds, i.e. the error bounds are given by equation (70) at period $T, T-1, \ldots, t+1$. We now want to show that it also holds at period t. We have

$$V_t(s) = \max_{d \in D_t(s)} \left[u_t(d, c_t(d, s), s) + \beta \int V_{t+1}(s') p_{t+1}(\partial s' | d, c_t(d, s), s) \right], \tag{74}$$

and

$$EV_{\sigma,t}(s) = \sigma \log \left(\sum_{d \in D_t(s)} \exp \left\{ \frac{1}{\sigma} \left[u_t(d, c_{\sigma,t}(d, s), s) + \beta \int EV_{\sigma,t+1}(s') p_{t+1}(\partial s' | d, c_{\sigma,t}(d, s), s) \right] \right\} \right). \tag{75}$$

Note that $c_{\sigma,t}(d, s)$ is the choice-specific continuous decision rule for the perturbed problem. Define a function $\tilde{V}_t(s)$ by substituting $c_{\sigma,t}(d, s)$ for $c_t(d, s)$ in equation (74):

$$\tilde{V}_t(s) = \max_{d \in D_t(s)} \left[u_t(d, c_{\sigma,t}(d, s), s) + \beta \int V_{t+1}(s') p_{t+1}(\partial s' | d, c_{\sigma,t}(d, s), s) \right]. \tag{76}$$

Since $c_{\sigma,t}(d, s)$ is not necessarily an optimal choice-specific consumption for the unperturbed problem, it follows that

$$\tilde{V}_t(s) \leq V_t(s), \quad \forall s \in S. \tag{77}$$

Similarly define the function $\tilde{EV}_{\sigma,t}(s)$ by substituting the conditional expectation of V_{t+1} instead

of the conditional expectation of $EV_{\sigma,t+1}$ in the formula for $EV_{\sigma,t}(s)$ in equation (75). We have

$$E\tilde{V}_{\sigma,t}(s) = \sigma \log\left(\sum_{d\in D_t(s)} \exp\left\{\frac{1}{\sigma}\left[u_t(d, c_{\sigma,t}(d,s), s) + \beta \int V_{t+1}(s')p_{t+1}(\partial s'|d, c_{\sigma,t}(d,s), s)\right]\right\}\right). \tag{78}$$

Note that we can write

$$\begin{aligned} EV_{\sigma,t}(s) &= \sigma \log\left(\sum_{d\in D_t(s)} \exp\left\{\frac{1}{\sigma}\left[u_t(d, c_{\sigma,t}(d,s), s) + \beta \int V_{t+1}(s')p_{t+1}(\partial s'|d, c_{\sigma,t}(d,s), s)\right.\right.\right. \\ &\quad \left.\left.\left. + \beta \int [EV_{\sigma,t+1}(s') - V_{t+1}(s')]p_{t+1}(\partial s'|s, c_{\sigma,t}(d,s), s)\right]\right\}\right). \end{aligned} \tag{79}$$

By the inductive hypothesis, it follows that

$$\beta \int [EV_{\sigma,t+1}(s') - V_{t+1}(s')]p_{t+1}(\partial s'|d, c_{\sigma,t}(d,s), s) \leq \sigma\beta\left[\sum_{j=0}^{T-t-1} \beta^j\right]\log(D). \tag{80}$$

Thus, it follows from inequality (80) that the following inequality holds

$$EV_{\sigma,t}(s) \leq E\tilde{V}_{\sigma,t}(s) + \sigma\beta\left[\sum_{j=0}^{T-t-1} \beta^j\right]\log(D). \tag{81}$$

From Lemma 2 we have

$$E\tilde{V}_{\sigma,t}(s) - \tilde{V}_t(s) \leq \sigma\log(D). \tag{82}$$

Using inequalities (77) and (82) it follows that

$$0 \leq EV_{\sigma,t}(s) - V_t(s) \leq \sigma\left[\sum_{j=0}^{T-t} \beta^j\right]\log(D), \tag{83}$$

completing the induction step of the argument. It follows by mathematical induction that inequality (70) holds for all $t \in \{0, 1, \ldots, T\}$ so Lemma 3 is proved. □

Note that the bound (70) is *uniform* over all states $s \in S$ since the right hand side of inequality does not depend on s. In particular, we do not need to rely on any continuity or boundedness assumptions about $V_t(s)$: this function could potentially be non-smooth or even discontinuous in s and an unbounded function of s, something typical in many economic problems with consumption and saving, including the retirement problem we analyzed in Section 2.

It follows from uniformity of bound (70) that (68) holds.

We turn now to establishing that the decision rules $\delta_{\sigma,t}(s,\varepsilon)$ and $c_{\sigma,t}(s,\varepsilon)$ in the perturbed problem converge the optimal decision rules $\delta_t(s)$ and $c_t(s)$ in the limiting unperturbed DP problem for $t \in \{0, 1, \ldots, T\}$. We will allow for the possibility that there are multiple values of d and c that attain the optimum values in equations (47) and (48) above, so in general we can interpret $c_t(s)$ and $\delta_t(s)$ as *correspondences* (i.e. set-valued functions of s). However the pointwise argument is simplest in the case where there is a unique discrete and continuous decision attaining the optimum so we first present the argument in this case in Lemma 4 below.

Lemma 4 (Policy convergence 1)**.** *Consider a point $s \in S$ for which $\delta_t(s)$ is just a single element $d \in D_t(s)$ and $c_t(s)$ is a single element of the set of feasible continuous choice $C_t(\delta_t(s), s)$ that attains the optimum. Then for* (69) *holds for any $\varepsilon \in R^D$.*

Since the pair of decisions $(\delta_t(s), c_t(s))$ is the unique optimizer of the Bellman equation in state $s \in S$, we have

$$\begin{aligned} & u_t(\delta_t(s), c_t(s), s) + \beta \int V_{t+1}(s') p_{t+1}(\partial s' | \delta_t(s), c_t(s), s) \\ = \; & u_t(\delta_t(s), c_t(\delta_t(s), s), s) + \beta \int V_{t+1}(s') p_{t+1}(\partial s' | \delta_t(s), c_t(\delta_t(s), s), s) \\ > \; & u_t(d, c, s) + \beta \int V_{t+1}(s') p_{t+1}(\partial s' | d, c, s) \quad \forall c \neq c_t(s) \in C_t(d, s), \; d \neq \delta_t(s) \in D_t(s). \end{aligned} \tag{84}$$

Let d be any limit point of the sequence $\{\delta_{\sigma,t}(s, \varepsilon)\}$. Since feasibility requires $\delta_{\sigma,t}(s, \varepsilon) \in D_t(s)$ and $D_t(s)$ is a finite set, at least one limit point must exist. Similarly let c be a limit point of the choice-specific continuous decision rule $c_{\delta,t}(\delta_{\sigma,t}(s, \varepsilon), s, \varepsilon)$. This also must have one limit point since feasibility requires that $c_{\sigma,t}(s, \varepsilon) = c_{\sigma,t}(\delta_{\sigma,t}(s, \varepsilon), s, \varepsilon) \in C_t(\delta_t(s, \varepsilon), s)$ where the latter is a compact set due to Assumption C (for any fixed d, however since we are considering a subsequence $\{\delta_{\sigma,t}(s, \varepsilon)\}$ that converges to a fixed point $d \in D_t(s)$ it follows the σ sufficiently small, the sequence of consumptions must be elements of the single compact set $C_t(d, s)$).

Now we show that $d = \delta_t(s)$ and $c = c_t(s)$ since otherwise we would have a contradiction of the strict optimality of the decisions $(\delta_t(s), c_t(s))$ in inequality (84). We have

$$\begin{aligned} EV_{\sigma,t}(s) &= \sigma \log \left(\sum_{d \in D_t(s)} \exp \left\{ \frac{1}{\sigma} \left[u_t(d, c_{\sigma,t}(d, s), s) + \beta \int EV_{\sigma,t+1}(s') p_{t+1}(\partial s' | d, c_{\sigma,t}(d, s), s) \right] \right\} \right) \\ &= \int V_{\sigma,t}(s, \varepsilon) F(\varepsilon) \\ &= \int \Big[u_t(\delta_{\sigma,t}(s, \varepsilon), c_{\sigma,t}(\delta_{\sigma,t}(s, \varepsilon), s), s) + \sigma \varepsilon(\delta_{\sigma,t}(s, \varepsilon) \\ &+ \beta \int EV_{\sigma,t+1}(s') p_{t+1}(\partial s' | \delta_{\sigma,t}(s, \varepsilon), c_{\sigma,t}(\delta_{\sigma,t}(s, \varepsilon), s) \Big] F(\varepsilon) \end{aligned} \tag{85}$$

By Lemma 3 we have that uniformly for each $t \in \{0, 1, \ldots, T\}$ and all $s \in S$

$$\lim_{\sigma \downarrow 0} EV_{\sigma,t}(s) = V_t(s). \tag{86}$$

However using the fact that for a susequence $\{\sigma_n\}$ converging to zero we have

$$\begin{aligned} \lim_{\sigma_n \downarrow 0} \delta_{\sigma_n,t}(s, \varepsilon) &= d \\ \lim_{\sigma_n \downarrow 0} c_{\sigma,t}(\delta_{\sigma,t}(s, \varepsilon), s) &= c \end{aligned} \tag{87}$$

these limits together with the representation of $EV_{\sigma,t}(s)$ in the last equation of (85) implies that

$$V_t(s) = u_t(d, c, s) + \beta \int V_{t+1}(s') p_{t+1}(\partial s' | d, c, s) \tag{88}$$

However because $\delta_t(s)$ and $c_t(s)$ are the unique optimizers of Bellman equation in equation (84) above, it follows that $d = \delta_t(s)$ and $c = c_t(s)$. This argument holds for all cluster points of $\{\delta_{\sigma,t}(s,\varepsilon)\}$ and $\{c_{\sigma,t}(s,\varepsilon)\}$ so it follows that for any sequence $\{\sigma_n\}$ with $\lim_n \sigma_n = 0$, the sequences $\{\delta_{\sigma_n,t}(s,\varepsilon)\}$ and $\{c_{\sigma_n,t}(s,\varepsilon)\}$ converge to $\delta_t(s)$ and $c_t(s)$, respectively, proving that the claimed limits in equation (69) the statement of Lemma 4 hold. □

Finally we consider the case where $\delta_t(s)$ and/or $c_t(s)$ are not singletons. We also allow for the optimal decision rules to the perturbed problem, $\delta_{\sigma,t}(s,\varepsilon)$ and $c_{\sigma,t}(s,\varepsilon)$ to be correspondences (corresponding to case where multiple choices attain the optimum in the Bellman equation) the fact that the extreme value taste shocks are continuously distributed over the entire real line implies that for almost all ε $\delta_{\sigma,t}(s,\varepsilon)$ will be a singleton (i.e. there will be a unique discrete choice that maximizes the agent's utility).

We now show in Lemma 5 that even when we allow for nonuniqueness in the optimizing choices of (d,c) in both the perturbed problem and the limiting unperturbed problem, the correspondences $\delta_{\sigma,t}(s,\varepsilon)$ and $c_{\sigma,t}(s,\varepsilon)$ are *upper hemicontinuous,* that is if we have limits given by

$$\begin{aligned} \lim_{\sigma\downarrow 0} \delta_{\sigma,t}(s,\varepsilon) &= d \\ \lim_{\sigma\downarrow 0} c_{\sigma,t}(s,\varepsilon) &= c \end{aligned} \tag{89}$$

where we now allow for the possibility that the limits d and c are actual *sets,* upper hemicontinuity requres that $d \subset \delta_t(s)$ and $c \subset c_t(s)$.

Lemma 5 (Policy convergence 2)**.** *Consider a point $s \in S$ where the decision rules $\delta_t(s)$ and $c_t(s)$ are potentially non-unique, i.e. these may be sets of points in $D_t(s)$ and $C_t(\delta_t(s),s)$, respectively. Then the correspondences $\delta_{\sigma,t}(s,\varepsilon)$ and $c_{\sigma,t}(s,\varepsilon)$ are upper hemicontinuous, and for almost all ε $\delta_{\sigma,t}(s,\varepsilon)$ is a singleton, which implies that its limit d is a single element in $\delta_t(s)$.*

The proof is similar to Lemma 4 except that we now allow for the possibility that in the limiting DP model without taste shocks, there may be multiple values of $d \in D_t(s)$ and $c \in C_t(\delta_t(s),s)$ that attain the maximum of the Bellman equation in equations (47) and (48) above. Since the extreme value distribution is continuous the probability that there are any ties in the perturbed DP problem with taste shocks is zero (with respect to the extreme value distribution) and thus for almost all (s,ε) $\delta_{\sigma,t}(s,\varepsilon)$ is a singleton, and thus its limit d is a singleton. Following the reasoning of Lemma 4, if c is a limit point of $c_{\sigma,t}(s,\varepsilon)$ as $\sigma \to 0$ we can represent c as

$$c \in \lim_{\sigma\downarrow 0} c_{\sigma,t}(d,s), \tag{90}$$

that is, c is one of the limit points of the $\{c_{\sigma,t}(s,\varepsilon)\}$. Now suppose that the pair (d,c) is not optimal, i.e. $d \neq \delta_t(s)$ and $c \notin c_t(s)$. Then following the same argument as in Lemma4 we can obtain a contradiction, because following the same argument we can show that equation (88) holds, but if (d,c) are not optimal, this would contradict the fact that $V_t(s)$ attains the maximum over all feasible (d,c) values in equations (47) and (48). □

This concludes the proof of Theorem 2. □

References

Adda, J., C. Dustmann and K. Stevens (forthcoming): "The Career Costs of Children," *Journal of Political Economy*.

Aguirregabiria, V. and P. Mira (2010): "Dynamic discrete choice structural models: A survey," *Journal of Econometrics*, 156(1), 38 – 67, Structural Models of Optimization Behavior in Labor, Aging, and Health.

Ameriks, J., J. S. Briggs, A. Caplin, M. D. Shapiro and C. Tonetti (2015): "Long-Term Care Utility and Late in Life Saving," Working Paper 20973, National Bureau of Economic Research.

Barillas, F. and J. Fernández-Villaverde (2007): "A generalization of the endogenous grid method," *Journal of Economic Dynamics and Control*, 31(8), 2698–2712.

Bertsekas, D. P., Y. Lee, B. van Roy and J. N. Tsitsiklis (1997): "A neuro-dynamic programming approach to retailer inventory management," in *Proceedings of the IEEE Conference on Decision and Control*, vol. 4, pp. 4052–4057.

Bound, J., T. Stinebrickner and T. Waidmann (2010): "Health, economic resources and the work decisions of older men," *Journal of Econometrics*, 156(1), 106–129.

Carroll, C. D. (2006): "The Method of Endogenous Gridpoints for Solving Dynamic Stochastic Optimization Problems," *Economics Letters*, 91(3), 312–320.

Carroll, C. D. and W. Dunn (1997): "Data Sources and Solution Methods for Unemployment expectations, jumping (S, s) triggers, and household balance sheets," in *NBER Macroeconomics Annual*, vol. 12, pp. 165–230. National Bureau of Economic Research, Inc.

Casanova, M. (2010): "Happy Together: A Structural Model of Couples' Joint Retirement Choices," Working paper, Department of Economics, UCLA.

Clausen, A. and C. Strub (2013): "A General and Intuitive Envelope Theorem," Working Paper 248, Edinburgh School of Economics.

Druedahl, J. and C. N. Jørgensen (2015): "Precautionary Borrowing and the Credit Card Debt Puzzle," Unpublished working paper, Department of Economics, University of Copenhagen.

Druedahl, J. and T. H. Jørgensen (2016): "A General Endogenous Grid Method for Multi-Dimensional Models with Non-Convexities and Constraints," Discussion paper 16-09, Department of Economics, University of Copenhagen.

Ejrnæs, M. and T. H. Jørgensen (2015): "Saving Behavior around Intended and Unintended Childbirths," unpublished mimeo, University of Copenhagen.

Fella, G. (2014): "A generalized endogenous grid method for non-smooth and non-concave problems," *Review of Economic Dynamics*, 17(2), 329–344.

French, E. and J. B. Jones (2011): "The Effects of Health Insurance and Self-Insurance on Retirement Behavior," *Econometrica*, 79(3), 69–732.

Gourinchas, P.-O. and J. A. Parker (2002): "Consumption over the life cycle," *Econometrica*, 70(1), 47–89.

Hakansson, N. H. (1970): "Optimal Investment and Consumption Strategies Under Risk for a Class of Utility Functions," *Econometrica*, 38-5, 587–607.

Hershberger, J. (1989): "Finding the upper envelope of n line segments in O(n log n) time," *Information Processing Letters*, 33(4), 169–174.

Hintermaier, T. and W. Koeniger (2010): "The method of endogenous gridpoints with occasionally binding constraints among endogenous variables," *Journal of Economic Dynamics and Control*, 34(10), 2074–2088.

Imai, S. and M. P. Keane (2004): "Intertemporal labor supply and human capital accumulation," *International Economic Review*, 45(2), 601–641.

Iskhakov, F. (2015): "Multidimensional endogenous gridpoint method: Solving triangular dynamic stochastic optimization problems without root-finding operations," *Economics Letters*, 135, 72 – 76.

Iskhakov, F. and M. Keane (2016): "An Analysis of the Australian Social Security System using a Life-Cycle Model of Labor Supply with Asset Accumulation and Human Capital," unpublished mimeo, University of New South Wales.

Jørgensen, T. H. (2013): "Structural estimation of continuous choice models: Evaluating the EGM and MPEC," *Economics Letters*, 119(3), 287–290.

——— (2014): "Leisure Complementarities in Retirement," mimeo, University of Copenhagen.

Ljungqvist, L. and T. Sargent (2005): "Lotteries for Consumers versus Lotteries for Firms," in *Frontiers in Applied General Equilibrium Modeling: in Honor of Herbert Scarf*, ed. by T. Kehoe, T. Srinivasan and J. Whalley, pp. 95–118. Cambridge University Press.

Ludwig, A. and M. Schön (2013): "Endogenous Grids in Higher Dimensions: Delaunay Interpolation and Hybrid Methods," Working Paper 65, University of Cologne.

McFadden, D. (1973): "Conditional logit analysis of qualitative choice behavior," in *Frontiers in econometrics*, ed. by P. Zarembka. Academic Press, New York.

Meghir, C. and L. Pistaferri (2004): "Income variance dynamics and heterogeneity," *Econometrica*, 72(1), 1–32.

Milgrom, P. and C. Shannon (1994): "Monotone Comparative Statics," *Econometrica*, 62(1), 157–80.

Oswald, F. (2016): "Regional Shocks, Migration and Homeownership," Unpublished working paper, Science Po.

Phelps, E. (1962): "The Accumulation of Risky Capital: A Sequential Utility Analysis," *Econometrica*, 30-4, 729–743.

Powell, W. B. (2007): *Approximate Dynamic Programming: Solving the curses of dimensionality*, vol. 703. John Wiley & Sons.

Prescott, E. (2005): "Nonconvexities in Quantitative General Equilibrium Studies of Business Cycles," in *Frontiers in Applied General Equilibrium Modeling: in Honor of Herbert Scarf*, ed. by T. Kehoe, T. Srinivasan and J. Whalley, pp. 95–118. Cambridge University Press.

Rogerson, R. (1988): "Indivisible Labor, Lotteries, and Equilibrium," *Journal of Monetary Economics*, 21, 3–16.

Rust, J. (1987): "Optimal Replacement of GMC Bus Engines: An Empirical Model of Harold Zurcher," *Econometrica*, 55(5), 999–1033.

——— (1988): "Maximum Likelihood Estimation of Discrete Control Processes," *SIAM Journal on Control and Optimization*, 26(5), 1006–1023.

Rust, J. (1994): "Structural estimation of Markov decision processes," in *Handbook of Econometrics, Vol. 4*, ed. by D. M. R. Engle, vol. chap. 51, pp. 3081–3143. Elsevier Science B.V., Amsterdam.

White, M. N. (2015): "The Method of Endogenous Gridpoints in Theory and Practice," *Journal of Economic Dynamics & Control*, 60, 26–41.

Yao, J., A. Fagereng and G. Natvik (2015): "Housing, Debt and the Marginal Propensity to Consume," Unpublished working paper, Johns Hopkins.